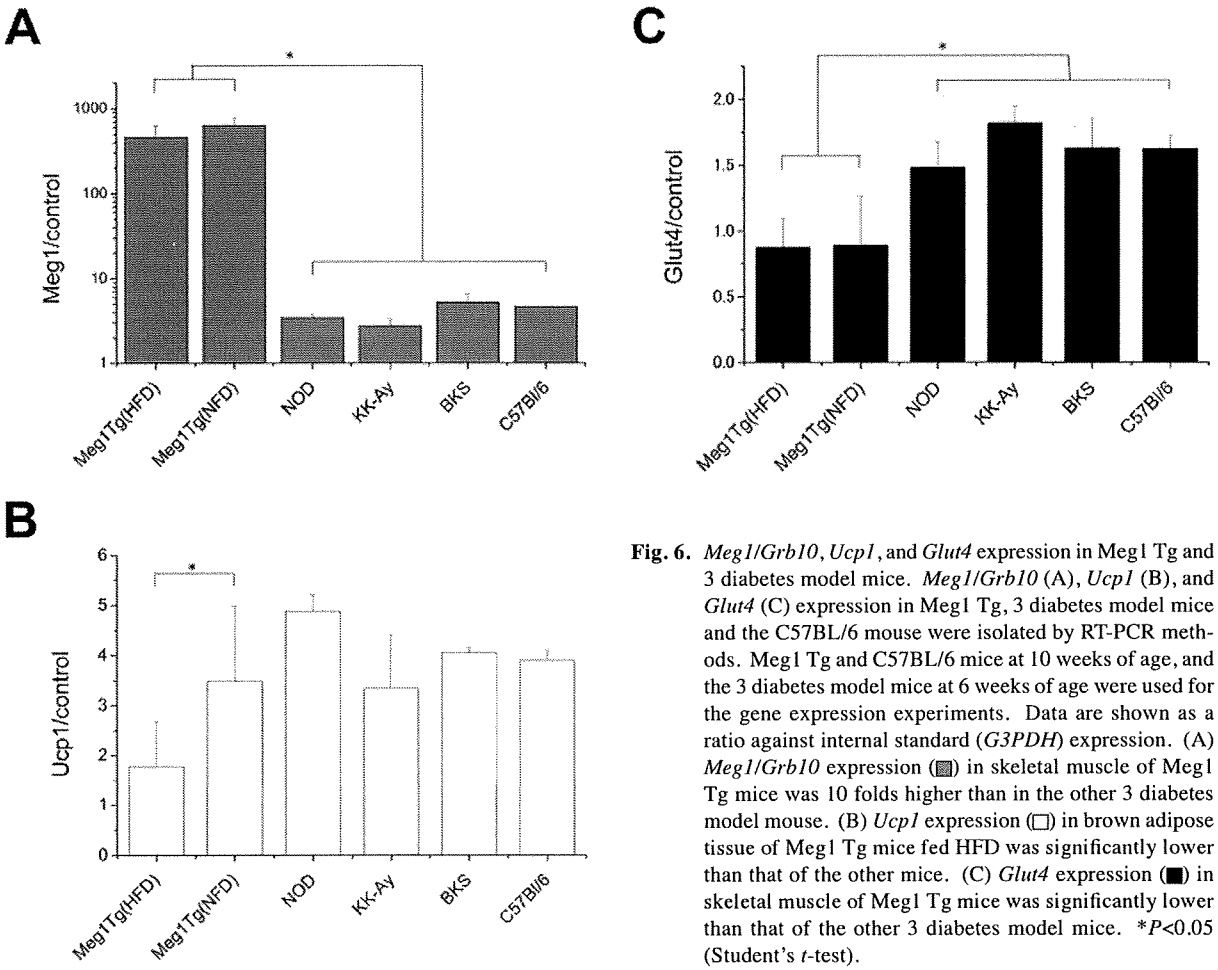

Fig. 6. *Meg1/Grb10*, *Ucp1*, and *Glut4* expression in Meg1 Tg and 3 diabetes model mice. *Meg1/Grb10* (A), *Ucp1* (B), and *Glut4* (C) expression in Meg1 Tg, 3 diabetes model mice and the C57BL/6 mouse were isolated by RT-PCR methods. Meg1 Tg and C57BL/6 mice at 10 weeks of age, and the 3 diabetes model mice at 6 weeks of age were used for the gene expression experiments. Data are shown as a ratio against internal standard (*G3PDH*) expression. (A) *Meg1/Grb10* expression (▩) in skeletal muscle of Meg1 Tg mice was 10 folds higher than in the other 3 diabetes model mouse. (B) *Ucp1* expression (□) in brown adipose tissue of Meg1 Tg mice fed HFD was significantly lower than that of the other mice. (C) *Glut4* expression (■) in skeletal muscle of Meg1 Tg mice was significantly lower than that of the other 3 diabetes model mice. $*P<0.05$ (Student's *t*-test).

ance (Fig. 3). The plasma insulin concentration of Meg1 Tg mice was significantly higher than in control mouse (Table 2). These data demonstrate that the dysregulation of plasma glucose was caused by insulin resistance. Our results provide support for Meg1 Tg mouse as a 2DM mouse model. Moreover, the body weights of Meg1 Tg neonates were slightly lower than controls, and this difference increased with growth up to 12 to 15% of body weight. BMI of Meg1 Tg mice was also smaller than control mice (Figs. 1 and 2). Body, visceral fat weight and liver weights were also slightly lower in Meg1 Tg mice than in control mice. However, the visceral fat/body weight and liver/body weight ratios of Meg1 Tg mice were similar to those of control mice (Table 1). Overall, the Meg1 Tg mouse showed a non-obese mouse character.

There are several spontaneous polygenic models of 2DM, such as the OLETF rat, the KK-A^y mouse, the NSY mouse, and the BKS mouse, which develop overt obesity and hyperinsulinemia prior to the onset of diabetes [7, 14, 34]. The KK-A^y mouse and the BKS mouse showed obesity compared with controls [33, 35]. However, the Meg1 Tg mouse model showed a non-obese character. Only limited data exist for 2DM in Japanese subjects, probably because Japanese people are relatively lean. Some Japanese 2DM patients are non-obese patients and the causal factors of 2DM onset is being analyze by many laboratories [15, 28]. The Meg1 Tg diabetes mouse model may provide a useful tool for these researches.

Biochemical analysis data of the Meg1 Tg mouse demonstrated metabolic abnormality. Plasma BUN in

Meg1 Tg mice was significantly lower than in control mice. Plasma TG, insulin, adiponectin, and resistin levels of HFD-fed Meg1 Tg mice were significantly higher than those of control mice. The mean concentration of TG in Meg1 Tg mice, especially with HFD feeding, was over 200 mg/dl, a condition that is called high-fat plasma. High-fat plasma is said to be a precursor of diabetes [19]. A high level of plasma adiponectin and low BMI were found in Meg1 Tg mice fed HFD (Fig. 2B). There was an inverse correlation between plasma adiponectin and BMI in the Meg1 Tg mouse (data not shown). This shows that the Meg1 Tg mouse has characteristics similar to human 2DM. The circulating IGF-1 level in Meg1 Tg mice tended to be lower than that of control mice (Table 2). A lower IGF-1 level could explain the lower body weight of the Meg1 Tg mouse due to the role of IGF-1 signaling in postnatal growth [10]. Overall, the biochemical data suggest that HFD feeding in the Meg1 Tg mouse induces human 2DM related characteristics. In a comparison of the biochemical data between the Meg1 Tg mouse and other 2DM model mice, such as KK-A^y and BKS mouse, the Meg1 Tg mouse did not show plasma insulin and a remarkable rise of plasma glucose levels like KK-A^y and BKS mice, but showed a property that is characteristic of human 2DM, a rise of adiponectin level [5, 16, 18]. In addition, it is a very unique characteristic that this property is caused by environmental factors such as diet.

In mRNA expression analysis, diabetes related genes, such as *Grb10*, *Ucp1*, and *Glut4*, in the Meg1 Tg mouse were compared with 3 famous diabetes mouse models (Fig. 6). Regarding the relationship between the *Meg1/Grb10* gene and the non-obese character of the Meg1 Tg mouse, overexpression of the *Meg1/Grb10* gene may hold the IGF-1 acceptor signal transduction system in check during development in the embryonic stage and the holding effect would be maintained until long after birth [31]. It is reported that maternal duplication of proximal chromosome 11 retards embryonic growth, whereas paternal duplication promotes growth [2]. A recent *Grb10* knockout study has clearly demonstrated that *Meg1/Grb10* is the gene responsible for embryonic overgrowth observed in paternal duplication of the chromosome 11 region [3], although the effect of *Meg1/Grb10* overproduction remains to be addressed. Our data may provide answers to these puzzling issues. Grb10 regulates the insulin signaling and sensitivity *in vivo* [36]. This suggests that a high level of the *Grb10* gene could affect insulin resistance in the Meg1 Tg mouse. The reduction in intracellular lipid by constitutive expression of *Ucp1* reflects down-regulation of fat synthesis rather than up-regulation of fatty acid oxidation [32]. The down-regulation of *Ucp1* in Meg1Tg mice fed HFD could explain the non-obese character of the Meg1 Tg mouse. The quantity of expression of *Glut4* mRNA in skeletal muscle decreased significantly in Meg1 Tg mice (Fig. 6C). GLUT4 translocation can be activated by insulin, to which the Meg1 Tg mouse has resistance, and may be related to the GLUT4 decrease in skeletal muscle.

Recently, association of hGrb10 genetic variations with 2DM in Caucasian subjects has been reported [2]. There is no evidence of such a correlation in Japanese subjects. However, it has been revealed that the expression of hGrb10 was influenced by epigenetic alterations. It is important to investigate hGrb10 expression and the relationship to environmental conditions including diet in 2DM model mice.

Acknowledgment(s)

We thank Ms. Tomoko Hata and Naho Takekawa for technical assistance.

References

1. Caroline, S.F., Michael, J.P., James, B.M., Ramachandran, S.V., Yamini, S.L., and Ralph, B.D. 2006. Trends in the incidence of type 2 diabetes mellitus from the 1970s to the 1990s. *Circulation* 113: 2914–2918.
2. Cattanach, B.M., Beechey, C.V., Rasberry, C., Jones J., and Papworth, D. 1996. Time of initiation and site of action of the mouse chromosome 11 imprinting effects. *Genet. Res.* 68: 35–44.
3. Charalambous, M., Smith, F.M., Bennett, W.R., Crew, T.E., Mackenzie, F., and Ward, A. 2003. Disruption of the imprinted *Grb10* gene leads to disproportionate overgrowth by an Igf2-independent mechanism. *Proc. Natl. Acad. Sci. U.S.A.* 100: 8292–8297.
4. Chu, K.Y., Lau, T., Carlsson, P.O., and Leung, P.S. 2006. Angiotensin II type 1 receptor blockade improves beta-cell function and glucose tolerance in a mouse model of type 2 diabetes. *Diabetes* 55: 367–374.
5. Combs, T.P., Wagner, J.A., Berger, J., Doebber, T., Wang,

W.-J., Zhang, B.B., Tanen, M., Berg, A.H., O'Rahilly, S., Savage, D.B., Chatterjee, K., Weiss, S., Larson, P.J., Gottesdiener, K.M., Gertz, B.J., Charron, M.J., Scherer, P.E., and Moller, D.E. 2002. Induction of adipocyte complement-related protein of 30 kilodaltons by PPARg agonists: a potential mechanism of insulin sensitization. *Endocrinology* 143: 998–1007.

6. Cramer, K.L., Gerrald, Q.D., Nichols, C.B., Price, M.S., and Alspaugh, J.A. 2006. Transcription factor Nrg1 mediates capsule formation, stress response, and pathogenesis in Cryptococcus neoformans. *Eukaryotic Cell* 5: 1147–1156.
7. DeChhiara, T.M., Robertson, E.J., and Efstratiadis, A. 1991. Parental imprinting of the mouse insulin-like growth factor II gene. *Cell* 64: 849–859.
8. Dey, B.R., Frick, K., Lopaczynski, W., Nissley, S.P., and Furlanetto, R.W. 1996. Evidence for the direct interaction of the insulin-like growth factor I receptor with IRS-1, Shc, and Grb10. *Mol. Endocrinol.* 10: 631–641.
9. Dong, L.Q., Du, H., Porter, S.G., Kolakowski, L.F., Lee, A.V., Mandarino, L.J., Fan, J., Yee, D., Liu, F., and Mandarino, J. 1997. Cloning, chromosome localization, expression, and characterization of an *Src* homology 2 and pleckstrin homology domain-containing insulin receptor binding protein hGrb10gamma. *J. Biol. Chem.* 272: 29104–29112.
10. Floria, L., Joseph, D.T., Kaechoong, L., Gino, V.S., Argiris, E. 2001. Roles of growth hormone and insulin-like growth factor 1 in mouse postnatal growth. *Dev. Biol.* 229: 141–162.
11. Furuya, Y., Tagami, S., Hasegawa, A., Ishii, J., Hirokawa, J., Yoshimura, H., Honda, T., Sakaue, S., Aoki, K., Murakami, M., Kudo, I., and Kawakami, Y. 1999. Increased glomerular cytosolic phospholipase A2 activity of OLETF rats with early diabetes. *Exp. Clin. Endocrinol. Diabetes* 107: 299–305.
12. Hanley, A.J., Karter, A.J., Williams, K., Festa, A., D'Agostino, R.B. Jr., Wagenknecht, L.E., and Haffner, S.M. 2005. Prediction of type 2 diabetes mellitus with alternative definitions of the metabolic syndrome: the Insulin Resistance Atherosclerosis Study. *Circulation* 112: 3675–3676.
13. Hattersley, A.T. 2004. Unlocking the secrets of the pancreatic beta cell: man and mouse provide the key. *J. Clin. Invest.* 114: 314–316.
14. Horio, F., Teradaira, S., Imamura, T., Anunciado, R.V., Kobayashi, M., Namikawa, T., and Niki, I. 2005. The HND mouse, a nonobese model of type 2 diabetes mellitus with impaired insulin secretion. *Eur. J. Endocrinol.* 153: 971–979.
15. Kanauchi, M. 2003. Comparison in renal histology between Japanese obese and non-obese microalbuminuric type 2 diabetic patients. *Nephrol. Dial. Transplant.* 18: 849–850.
16. Kawasaki, F., Matsuda, M., Kanda, Y., Inoue, H., and Kaku, K. 2005. Structural and functional analysis of pancreatic islets preserved by pioglitazone in *db/db* mice. *Am. J. Physiol. Endocrinol. Metab.* 288: E510–E518.
17. Kushi, A., Sasai, H., Koizumi, H., Takeda, N., Yokoyama, M., and Nakamura, M. 2006. Obesity and mild hyperinsulinemia found in neuropeptide Y-Y1 receptor-deficient mouse. *Proc. Natl. Acad. Sci. U.S.A.* 95: 15659–15664.
18. Kuwabara, K., Murakami, K., Todo, M., Aoki, T., Asaki, T., Murai, M., and Yano, J. 2004. A novel selective peroxisome proliferator-activated receptor a agonist, 2-methyl-c-5-[4-[5-methyl-2-(4-methyphenyl)-4-oxazolyl]butyl]-1,3-dioxane-r-2-carboxylic acid(NS-220), potently decreases plasma triglyceride and glucose levels and modifies lipoprotein profiles in KK-A^y mice. *J. Pharmacol. Exp. Ther.* 309: 970–977.
19. Lewis, G.F., O'Meara, N.M., Soltys, P.A., Blackman, J.D., Iverius, P.H., Pugh, W.L., Getz, G.S., and Polonsky, K.S. 1991. Fasting hypertriglyceridemia in noninsulin-dependent diabetes mellitus is an important predictor of postprandial lipid and lipoprotein abnormalities. *J. Clin. Endocrinol. Metab.* 72: 934–944.
20. Louvi, A., Accili, D., and Efstratiadis, A. 1997. Growth-promoting interaction of IGF-II with the insulin receptor during mouse embryonic development. *Dev. Biol.* 189: 33–48.
21. Ma, D., Shield, J.P., Dean, W., Leclerc, I., Knauf, C., Burcelin, R.R., Rutter, G.A., and Kelsey, G. 2004. Impaired glucose homeostasis in transgenic mouse expressing the human transient neonatal diabetes mellitus locus, TNDM. *J. Clin. Invest.* 114: 339–348.
22. Miao, G., Ito, T., Uchikoshi, F., Tanemura, M., Kawamoto, K., Shimada, K., Nozawa, M., and Matsuda, H. 2005. Development of islet-like cell clusters after pancreas transplantation in the spontaneously diabetic Torri rat. *Am. J. Transplant.* 5: 2360–2367.
23. Miyoshi, N., Kuroiwa, Y., Kohda, T., Shitara, H., Yonekawa, H., Kawabe, T., Hasegawa, H., Barton, S.C., Surani, M.A., Kaneko-Ishino, T., and Ishino, F. 1998. Identification of the *Meg1/Grb10* imprinted gene on mouse proximal chromosome 11, a candidate for the Silver–Russell syndrome gene. *Proc. Natl. Acad. Sci. U.S.A.* 95: 1102–1107.
24. Momose, K., Nunomiya, S., Nakata, M., Yada, T., Kikuchi, M., and Yashiro, T. 2006. Immunohistochemical and electron-microscopic observation of beta-cells in pancreatic islets of spontaneously diabetic Goto-Kakizaki rats. *Med. Mol. Morphol.* 39: 146–153.
25. Morrione, A., Valentinis, B., Resnicoff, M., Xu, S., and Baserga, R. 1997. The role of m*Grb10*alpha in insulin-like growth factor I-mediated growth. *J. Biol. Chem.* 272: 26382–26387.
26. Nakae, J., Kido, Y., and Accili, D. 2001. Distinct and overlapping functions of insulin and IGF-I receptors. *Endcr. Rev.* 22: 818–835.
27. O'Neill, T. J., Rose, D.W., Pillay, T.S., Hotta, K., Olefsky, J.M., and Gustafson, T.A. 1996. Interaction of a GRB-IR splice variant (a human GRB10 homolog) with the insulin and insulin-like growth factor I receptors. Evidence for a role in mitogenic signaling. *J. Biol. Chem.* 271: 22506–22513.
28. Ohki, Y., Kishi, M., Orimo, H., and Ohkawa, T. 2004. Insulin resistance in Japanese adolescents with type 2 diabetes mellitus. *J. Nippon Med. Sch.* 71: 88–91.
29. Paola, R.D., Ciociola, E., Boonyasrisawat, W., Nolan, D.,

Duffy, J., Miscio, G., Cisternino, C., Fini, G., Tassi, V., Doria, A., and Trischitta, V. 2006. Association of hGrb 10 genetic variations with type 2 diabetes in Caucasian subjects. *Diabetes Care* 29: 1181–1182.

30. Reynisdottir, I., Thorleifsson, G., Benediktsson, R., Sigurdsson, G., Emilsson, V., Einarsdottir, A.S., Hjorleifsdottir, E.E., Orlygsdottir, G.T., Bjornsdottir, G.T., Saemundsdottir, J., Halldorsson, S., Hrafnkelsdottir, S., Sigurjonsdottir, S.B., Steinsdottir, S., Martin, M., Kochan, J.P., Rhees, B.K., Grant, S.F., Frigge, M.L., Kong, A., Gudnason, V., Stefansson, K., and Gulcher, J.R. 2003. Localization of a susceptibility gene for type 2 diabetes to chromosome 5q34-q35.2. *Am. J. Hum. Genet.* 73: 323–335.
31. Shiura, H., Miyoshi, N., Konishi, A., Wakisaka-Saito, N., Suzuki, R., Muguruma, K., Kohda, T., Wakana, S., Yokoyama, M., Ishino, F., and Kaneko-Ishino, T. 2005. *Meg1/Grb10* overexpression causes postnatal growth retardation and insulin resistance via negative modulation of the IGF1R and IR cascades. *Biochem. Biophys. Res. Commun.* 329: 909–916.
32. Si, Y., Palani, S., Jayaraman, A., and Lee, K. 2007. Effects of forced uncoupling protein 1 expression in 3T3-L1 cells on mitochondrial function and lipid metabolism. *J. Lipid Res.* 48: 826–836.
33. Takada, Y., Takata, Y., Iwanishi, M., Imamura, T., Sawa, T., Morioka, H., Ishihara, H., Ishiki, M., Usui, I., Temaru, R., Urakaze, M., Satoh, Y., Inami, T., Tsuda, S., and Kobayashi, M. 1996. Effect of glimepiride (HOE 490) on insulin receptors of skeletal muscles from genetically diabetic KK-A^y mouse. *Eur. J. Pharmacol.* 308: 205–210.
34. Takeuchi, M., Itakura, A., Okada, M., Mizutan, S., and Kikkawa, F. 2006. Impaired insulin-regulated membrane aminopeptidase translocation to the plasma membrane in adipocytes of Otsuka Long Evans Tokushima Fatty rats. *Nagoya J. Med. Sci.* 68: 155–163.
35. Teixeira, S.R., Tappenden, K.A., and Erdman, J.W. Jr. 2003. Altering dietary protein type and quantity reduces urinary albumin excretion without affecting plasma glucose concentrations in BKS.Cg-+*Lepr^{db}*/+*Lepr^{db}* (*db/db*) mouse. *J. Nutr.* 133: 673–678.
36. Wang, L., Balas, B., Christ-Roberts, C.Y., Kim, R.Y., Ramos, F.J., Kikani, C.K., Li, C., Deng, C., Reyna, S., Musi, N., Dong, L.Q., DeFronzo, R.A., Liu, F. 2007. Peripheral disruption of the *Grb10* gene enhances insulin signaling and sensitivity *in vivo*. *Mol. Cell. Biol.* 27: 6497–6505.
37. Wright, N.M., Metzger, D.L., Borowitz, S.M., and Clarke, W.L. 1993. Permanet neonatal diabetes mellitus and pancreatic agenesis. *Am. J. Dis. Child.* 147: 607–609.
38. Yi, L.Z., He, J., Liang, Y.Z., Yuan, D.L., and Chau, F.T. 2006. Plasma fatty acid metabolic profiling and biomarkers of type 2 diabetes mellitus based on GC/MS and PLS-LDA. *FEBS Lett.* 580: 6837–6845.
39. 1999–2001 National Health Interview Survey and 1999–2000 National Health and Nutrition Examination Survey estimates projected to year 2002. National Diabetes Fact Sheet, National Estimates on Diabetes. CDC publications and products.

blood

2009 113: 5323-5329
Prepublished online Dec 24, 2008;
doi:10.1182/blood-2008-07-169359

The distal carboxyl-terminal domains of ADAMTS13 are required for regulation of in vivo thrombus formation

Fumiaki Banno, Anil K. Chauhan, Koichi Kokame, Jin Yang, Shigeki Miyata, Denisa D. Wagner and Toshiyuki Miyata

Blood (print ISSN 0006-4971, online ISSN 1528-0020), is published semimonthly by the American Society of Hematology, 1900 M St, NW, Suite 200, Washington DC 20036.

The distal carboxyl-terminal domains of ADAMTS13 are required for regulation of in vivo thrombus formation

Fumiaki Banno,[1] Anil K. Chauhan,[2,3] Koichi Kokame,[1] Jin Yang,[1] Shigeki Miyata,[4] Denisa D. Wagner,[2,3] and Toshiyuki Miyata[1]

[1]Research Institute, National Cardiovascular Center, Suita, Japan; [2]Immune Disease Institute and [3]Department of Pathology, Harvard Medical School, Boston, MA; and [4]Division of Transfusion Medicine, National Cardiovascular Center, Suita, Japan

ADAMTS13 is a multidomain protease that limits platelet thrombogenesis through the cleavage of von Willebrand factor (VWF). We previously identified 2 types of mouse *Adamts13* gene: the 129/Sv-strain *Adamts13* gene encodes the long-form ADAMTS13 having the same domains as human ADAMTS13, whereas the C57BL/6-strain *Adamts13* gene encodes the short-form ADAMTS13 lacking the distal C-terminal domains. To assess the physiologic significance of the distal C-terminal domains of ADAMTS13, we generated and analyzed 129/Sv-genetic background congenic mice (*Adamts13*$^{S/S}$) that carry the short-form ADAMTS13. Similar to wild-type 129/Sv mice (*Adamts13*$^{L/L}$), *Adamts13*$^{S/S}$ did not have ultralarge VWF multimers in plasma, in contrast to 129/Sv-genetic background ADAMTS13-deficient mice (*Adamts13*$^{-/-}$). However, in vitro thrombogenesis under flow at a shear rate of 5000 s^{-1} was accelerated in *Adamts13*$^{S/S}$ compared with *Adamts13*$^{L/L}$. Both in vivo thrombus formation in ferric chloride–injured arterioles and thrombocytopenia induced by collagen plus epinephrine challenge were more dramatic in *Adamts13*$^{S/S}$ than in *Adamts13*$^{L/L}$ but less than in *Adamts13*$^{-/-}$. These results suggested that the C-terminally truncated ADAMTS13 exhibited decreased activity in the cleavage of VWF under high shear rate. Role of the C-terminal domains may become increasingly important under prothrombotic conditions. (Blood. 2009;113:5323-5329)

Introduction

ADAMTS13 is a plasma protease that specifically cleaves von Willebrand factor (VWF).[1] VWF is a multimeric plasma glycoprotein that plays a critical role in platelet adhesion and aggregation on vascular lesions.[2] Endothelial cells and megakaryocytes produce mainly VWF as large multimers that can exceed 20 000 kDa in mass and secrete the multimers into the circulating blood. The adhesive activity of VWF multimers depends on their molecular sizes and in particular the largest multimers, called ultralarge VWF (UL-VWF) multimers, can induce excessive platelet aggregation under shear stress. UL-VWF multimers are normally cleaved by ADAMTS13 to smaller forms, thus restraining platelet thrombus formation. The lack of ADAMTS13 activity allows UL-VWF multimers to persist in the circulation and leads to the development of thrombotic thrombocytopenic purpura (TTP).[3-5]

ADAMTS13 consists of multiple domains including a metalloprotease domain, a disintegrin-like domain, a thrombospondin type 1 motif (Tsp1) domain, a cysteine-rich domain, a spacer domain, 7 additional Tsp1 domains and 2 complement components C1r/C1s, urchin epidermal growth factor, and bone morphogenic protein-1 (CUB) domains in order from the N-terminus. So far, the functional roles of ADAMTS13 domains have been studied using in vitro assay systems.[6-13] These studies have shown an essential role of the N-terminal region of ADAMTS13 from the metalloprotease domain to the spacer domain, on the VWF cleavage. However, the results from in vitro studies have lacked consistency on the relative importance of the C-terminal Tsp1 and CUB domains in the substrate recognition and the activity of ADAMTS13. The recombinant human ADAMTS13 mutant lacking the C-terminal Tsp1 and CUB domains maintain almost absolute VWF-cleaving activity under static conditions, indicating that the C-terminal domains are dispensable for the ADAMTS13 activity.[6-8] Under flow, the same mutant is hyperactive for the cleavage of newly released VWF multimers anchored on endothelial cells, suggesting that the C-terminal domains negatively regulate the activity of ADAMTS13.[10] Recombinant polypeptides and synthetic peptides derived from the first CUB domain can inhibit the cleavage of VWF multimers on endothelial cells by ADAMTS13 under flow.[11] Removal of the C-terminal Tsp1 and CUB domains results in a marked decrease in VWF cleavage by ADAMTS13 in a vortex mixer and in VWF binding to ADAMTS13 in a Biacore system (Uppsala, Sweden),[13] indicating that the C-terminal domains play a crucial role in the recognition and cleavage of VWF. These results prompted us to investigate the role of C-terminal domains of ADAMTS13 in vivo.

In laboratory mouse strains, 2 kinds of *Adamts13* gene are present.[14-16] The *Adamts13* gene of the 129/Sv strain contains 29 exons like the human *ADAMTS13* gene and encodes the full-length ADAMTS13 with the same domain constitutions as human ADAMTS13. On the other hand, several strains of mice, including the C57BL/6 strain, harbor the insertion of an intracisternal A-particle (IAP) retrotransposon into intron 23 of the *Adamts13* gene. As a result, the distal C-terminally truncated ADAMTS13 lacking the C-terminal 2 Tsp1 domains and 2 CUB domains is predominantly expressed in these strains. Therefore, mice can be suitable animal models for evaluating functions of the distal C-terminal domains, the C-terminal 2 Tsp1 domains, and 2 CUB domains, in vivo.

Submitted July 16, 2008; accepted December 16, 2008. Prepublished online as *Blood* First Edition paper, December 24, 2008; DOI 10.1182/blood-2008-07-169359.

The publication costs of this article were defrayed in part by page charge payment. Therefore, and solely to indicate this fact, this article is hereby marked "advertisement" in accordance with 18 USC section 1734.

An Inside *Blood* analysis of this article appears at the front of this issue.

In the present study, through using the spontaneous IAP insertion in mouse *Adamts13* gene, we generated a congenic mouse model that had the distal C-terminally truncated ADAMTS13 on 129/Sv genetic background. While comparing with wild-type 129/Sv mice having full-length ADAMTS13 and ADAMTS13-deficient mice on the same genetic background, we analyzed platelet thrombus formation in the congenic mice to define physiologic significance of the distal C-terminal domains in ADAMTS13 functions. Our results indicate that the distal C-terminal domains of ADAMTS13 contribute to the processing of VWF multimers in vivo, and that the importance of these domains becomes obvious after suffering thrombogenic stimuli.

Methods

Animals

The 129/Sv mice were purchased from Clea Japan (Tokyo, Japan). C57BL/6 mice were purchased from Japan SLC (Hamamatsu, Japan). ADAMTS13-deficient mice on the 129/Sv genetic background were described previously.[17,18] ADAMTS13-congenic mice were developed by introgressing the C57BL/6-*Adamts13* gene onto the 129/Sv genetic background, as follows. C57BL/6 mice were backcrossed to 129/Sv mice for 10 generations while retaining the C57BL/6-*Adamts13* gene. In the resulting N10 heterozygous mice, autosomal chromosomes were theoretically 99.9% identical to those of the 129/Sv strain and sex chromosomes were derived exclusively from the 129/Sv strain. The N10 heterozygous mice were interbred to produce homozygous mice. The *Adamts13*-genotype was determined by polymerase chain reaction (PCR) with HotStarTaq DNA polymerase (QIAGEN, Hilden, Germany). The amplification was carried out using primers: the intron 23-specific forward primer, 5′-ACCTCTCAAGTGTTTGGGATGCTA-3′, the IAP-specific reverse primer, 5′-TCAGCGCCATCTTGTGACGGCGAA-3′, and the primer downstream of the IAP target site, 5′-TGCCAGATGGCCATGATTAACTCT-3′. For the experiments, all animals were matched for age and sex. All animal procedures were approved by the Animal Care and Use Committees of the National Cardiovascular Center Research Institute and Immune Disease Institute.

Northern blot analysis

Total RNA was extracted from liver using ISOGEN reagent (Nippon Gene, Tokyo, Japan) and poly(A)$^+$ RNA was purified using PolyATtract mRNA Isolation Systems (Promega, Madison, WI). The alkaline phosphatase–labeled probe was synthesized from mouse *Adamts13* cDNA (1.3 kb) using AlkPhos Direct labeling module (GE Healthcare, Little Chalfont, United Kingdom). Poly(A)$^+$ RNA was separated on a 1% agarose gel containing 2% formaldehyde and transferred to a nylon membrane. The probe was hybridized to the blot and detected using CDP-Star detection reagent (GE Healthcare).

Blood sampling

Blood was collected from the retro-orbital plexus into tubes containing a 0.1 volume of 3.8% sodium citrate. Blood cell counts and hematocrit were determined using an automatic cell counter (KX-21NV; Sysmex, Kobe, Japan). Plasma was prepared from blood by centrifugation at 800*g* for 15 minutes.

Determination of plasma ADAMTS13 activity

Plasma ADAMTS13 activity was measured using GST-mVWF73-H, a recombinant mouse VWF73 peptide flanked by N-terminal glutathione S-transferase (GST) and C-terminal His_6 tags, as described previously.[14] In brief, GST-mVWF73-H (500 ng) was incubated with 0.8 μL plasma in 40 μL reaction buffer (10 mM *N*-2-hydroxyethylpiperazine-*N*′-2-ethanesulfonic acid, 150 mM NaCl, 5 mM $CaCl_2$, and 0.005% Tween 20, pH 7.4) at 37°C for 1 hour. The reaction was stopped by adding 10 μL sodium dodecyl sulfate (SDS) sample buffer (50 mM tris(hydeoxymethyl)aminomethane-HCl, 10 mM EDTA, 10% SDS, 250 mM dithiothreitol, 30% glycerol, and 0.1% bromophenol blue, pH 6.8). The samples were subjected to SDS–polyacrylamide gel electrophoresis and Western blot using a rabbit anti-GST antibody (Invitrogen, Carlsbad, CA) and a peroxidase-labeled anti–rabbit IgG antibody (KPL, Gaithersburg, MD). Activity was also determined using a fluorogenic human VWF73 peptide of FRETS-VWF73 (Peptide Institute, Minoh, Japan).[19,20] FRETS-VWF73 (2 μM) was incubated with 4 μL plasma in 200 μL assay buffer (5 mM bis(2-hydroxyethyl)-amino-tris(hydeoxymethyl)methane, 25 mM $CaCl_2$, and 0.005% Tween 20, pH 6.0) at 30°C. Increases in fluorescence were measured using a 350-nm excitation filter and a 440-nm emission filter in a fluorescence photometer (Mx3000P; Stratagene, La Jolla, CA).

VWF multimer analysis

Plasma VWF multimer patterns were analyzed as described previously.[17] Plasma samples in SDS sample buffer were electrophoresed on a 1% agarose gel (Agarose IEF; GE Healthcare) at a constant current of 15 mA at 4°C. After transfer to a nitrocellulose membrane, the membrane was incubated in peroxidase-conjugated rabbit anti–human VWF (1:500; Dako, Glostrup, Denmark) in 5% skim milk to detect VWF multimers. Bound antibody was detected with Western Lighting Chemiluminescence Reagent Plus (PerkinElmer, Waltham, MA) on an image analyzer (LAS-3000; Fujifilm, Tokyo, Japan). The chemiluminescent intensities of each lane were scanned using Image Gauge software (version 4.2.2; Fujifilm); the relative intensity profiles were shown.

Parallel plate flow chamber assay

Platelet thrombus formation in flowing blood on immobilized collagen was analyzed using a parallel plate flow chamber as described previously.[17,21] Acid-insoluble type I collagen–coated glass coverslips were placed in a flow chamber. The chamber was mounted on a fluorescence microscope (Axiovert 200M; Carl Zeiss, Oberkochen, Germany) equipped with a CCD camera system (DXC-390; Sony, Tokyo, Japan). Blood was collected into tubes containing argatroban (240 μM; Mitsubishi Chemical, Tokyo, Japan). The fluorescent dye mepacrine (10 μM; Sigma-Aldrich, St Louis, MO) was added to the blood. Whole blood samples were aspirated through the chamber and across the collagen-coated coverslip at a constant wall shear rate. To analyze the cumulative thrombus volume, image sets at 1.0-μm z-axis intervals within a defined area (156.4 μm × 119.6 μm) were captured using MetaMorph software (version 6.1.4; Universal Imaging, West Chester, PA). After blind deconvolution of image sets processed by AutoDeblur software package (version 8.0.2; AutoQuant Imaging, Troy, NY), 3D volumetric measurements of thrombi were accomplished using VoxBlast software (version 3.0; Vartek, Fairfield, IA).

Intravital microscopy

Intravital microscopy was performed as described previously.[22,23] Platelets were isolated from platelet-rich plasma and fluorescently labeled with calcein AM (2.5 μg/mL; Invitrogen). Recipient mice were anesthetized and labeled platelets were infused through retro-orbital plexus. The mesentery was gently exteriorized through a midline abdominal incision and arterioles of 100- to 150-μm diameters were visualized with a fluorescence microscope and a CCD camera system. The shear rate was calculated using an optical Doppler velocimeter as described.[24] Filter paper saturated with 10% ferric chloride was applied for 5 minutes on an arteriole by topical application. Thrombus formation in the arteriole was monitored for 40 minutes after injury or until complete occlusion occurred and lasted for more than 30 seconds. The following 2 parameters were evaluated: time to first thrombus formation, defined as the time required for formation of a thrombus larger than 30 μm, and occlusion time, defined as the time required for cessation of blood flow for at least 30 seconds.

Collagen plus epinephrine–induced thrombosis model

A mixture of 600 ng/g collagen (Nycomed, Roskilde, Denmark) and 60 ng/g epinephrine (Sigma-Aldrich) was infused into tail vein of mice.[17,25]

Blood was collected 5 minutes after the infusion and platelet counts were determined.

Statistical analysis

Statistical significance was assessed by the one-way analysis of variance followed by the Bonferroni multiple comparison tests. Differences were considered to be significant at P values less than .05.

Results

Generation of Adamts13$^{S/S}$ mice

To address the functional implication of the distal C-terminal domains of ADAMTS13 in vivo, we generated and characterized a congenic mouse model that has the C-terminally truncated form of ADAMTS13 on 129/Sv genetic background (Figure 1A). We confirmed the presence of IAP insertion in the *Adamts13* gene of the congenic (*Adamts13*$^{S/S}$) mice by PCR (data not shown) and detected an IAP chimeric transcript (~ 3.5 kb) by Northern blotting of RNA from liver (Figure 1B), primary site of synthesis.[14] An IAP-free ADAMTS13 mRNA (~ 5 kb) was detected in wild-type 129/Sv (*Adamts13*$^{L/L}$) mice and no ADAMTS13 mRNA was detected in ADAMTS13-deficient (*Adamts13*$^{-/-}$) mice on 129/Sv genetic background (Figure 1B). *Adamts13*$^{S/S}$ mouse plasma exhibited higher cleaving activity for both GST-mVWF73-H and FRETS-VWF73 than *Adamts13*$^{L/L}$ mouse plasma, whereas the activity in *Adamts13*$^{-/-}$ mouse plasma was below detection limits (Figure 1C,D). Therefore, the distal C-terminal domains of ADAMTS13 were not necessary for the cleavage of the VWF73-based peptide substrate as observed previously.[8,14] Platelet counts were not different among the genotypes (*Adamts13*$^{L/L}$, 744 ± 180 × 10^9/L; *Adamts13*$^{S/S}$, 693 ± 44 × 10^9/L; *Adamts13*$^{-/-}$, 672 ± 39 × 10^9/L; mean ± SD, n = 8). Both *Adamts13*$^{S/S}$ mice and *Adamts13*$^{-/-}$ mice were viable and showed no TTP-like symptoms throughout the study.

Adamts13$^{S/S}$ mice have normal VWF multimers

As previously reported,[17] UL-VWF multimers persisted in plasma of *Adamts13*$^{-/-}$ mice on 129/Sv-genetic background (Figure 2). Thus, ADAMTS13 activity is important for the size regulation of VWF multimers in mice at least on this genetic background. However, the VWF multimer patterns in *Adamts13*$^{S/S}$ mice were indistinguishable from those in *Adamts13*$^{L/L}$ mice (Figure 2). These results suggest that the distal C-terminally truncated form of mouse ADAMTS13 exhibits VWF-cleaving activity sufficient for maintenance of normal size distribution of plasma VWF multimers under steady state in vivo.

In vitro thrombogenesis is increased in *Adamts13*$^{S/S}$ mice only at a high shear rate

When whole blood was perfused over a collagen-coated surface in a parallel plate flow chamber at a shear rate of 1000 s^{-1}, platelet thrombus formation was significantly promoted in *Adamts13*$^{-/-}$ mice (Figure 3A) compared with *Adamts13*$^{L/L}$ mice, consistent with the presence of UL-VWF multimers in plasma of *Adamts13*$^{-/-}$ mice. However, whole blood thrombus formation at 1000 s^{-1} was not significantly different between *Adamts13*$^{S/S}$ mice and *Adamts13*$^{L/L}$ mice (Figure 3A), indicating that the distal C-terminally truncated form of mouse ADAMTS13 does not completely lose the activity.

As fluid shear rate increases progressively, the interaction between VWF and platelet GPIbα becomes more important in platelet thrombus formation.[26] It has been reported that thrombus formation in mouse blood on collagen surface is completely dependent on the VWF-GPIbα interaction above a threshold shear rate between 2000 s^{-1} and 5000 s^{-1}.[27] In addition, ADAMTS13 cleaves VWF and down-regulates thrombus formation in shear rate–dependent manner.[28] Based on these observations, we further examined thrombus formation at a higher shear rate of 5000 s^{-1}. As expected, thrombus formation in *Adamts13*$^{-/-}$ mice was significantly elevated compared with *Adamts13*$^{L/L}$ mice at 5000 s^{-1} (Figure 3B). In addition, we found accelerated thrombus formation in *Adamts13*$^{S/S}$ mice compared with *Adamts13*$^{L/L}$ mice at this higher shear rate (Figure 3B). These results suggest that the distal C-terminally truncated form of mouse ADAMTS13 has reduced

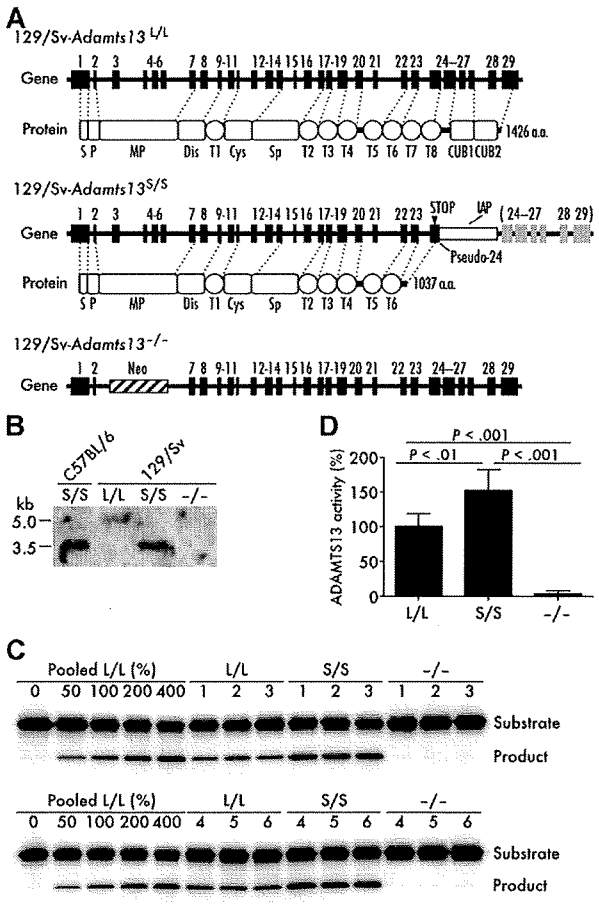

Figure 1. Generation of *Adamts13*$^{S/S}$ mice with 129/Sv-genetic background. (A) Gene and protein structure of ADAMTS13 in the wild-type (*Adamts13*$^{L/L}$) 129/Sv mice, the *Adamts13*$^{S/S}$ mice on 129/Sv genetic background, and the *Adamts13*$^{-/-}$ mice on 129/Sv genetic background. An intracisternal A-particle (*IAP*) insertion into intron 23 creates a pseudo-exon 24 including a premature stop codon. ADAMTS13 with a truncated C-terminus is expressed mainly in *Adamts13*$^{S/S}$ mice. S indicates signal peptide; P, propeptide; MP, metalloprotease domain; Dis, disintegrin-like domain; T (numbered 1-8), thrombospondin type 1 motif domain; Cys, cysteine-rich domain; Sp, spacer domain; and CUB, complement components C1r/C1s, urchin epidermal growth factor, and bone morphogenic protein-1 domain. (B) Expression of *Adamts13* mRNA in liver. Poly(A)$^+$ RNA isolated from liver of indicated mice was probed with a 1.3-kb Adamts13 cDNA corresponding to exons 3 to 13. (C) GST-mVWF73-H assay. Plasma ADAMTS13 activity of indicated mice was measured using a recombinant mouse VWF73 peptide, GST-mVWF73-H. Results from 6 mice for each genotype are shown. Standard reactions using graded amounts of pooled plasma from 10 *Adamts13*$^{L/L}$ mice were performed simultaneously. (D) FRETS-VWF73 assay. Plasma ADAMTS13 activity in indicated mice was determined using a fluorogenic human VWF73 peptide, FRETS-VWF73. Data are mean ± SD of 6 mice for each genotype. The average activity measured in *Adamts13*$^{L/L}$ mice was arbitrarily defined as 100%.

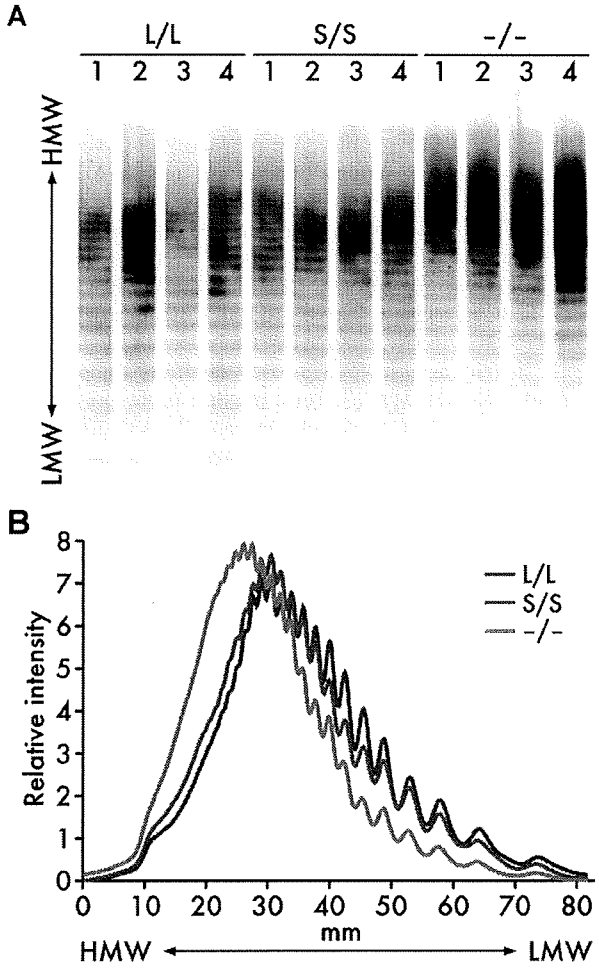

Figure 2. Plasma VWF multimers. (A) VWF multimer patterns. Plasma samples (1 μL/lane) from *Adamts13*$^{L/L}$, *Adamts13*$^{S/S}$, and *Adamts13*$^{-/-}$ mice were electrophoresed on SDS-agarose gels and transferred to nitrocellulose membranes. VWF multimers were detected with anti-VWF antibodies. (B) Relative intensities of plasma VWF multimers. The chemiluminescent intensities of the VWF multimer patterns (A) were scanned using image analysis software. An average of multiple lanes from 4 mice for each genotype is shown. HMW indicates high molecular weight; LMW, low molecular weight.

activity compared with the full-length form and does not sufficiently limit thrombus formation under high shear rate in vitro.

In vivo thrombus growth is accelerated in *Adamts13*$^{S/S}$ mice

To examine whether the truncation of the distal C-terminal domains in ADAMTS13 affects thrombus formation in vivo, we carried out intravital microscopy experiments in a model of experimental arteriolar thrombosis. In this model, vascular injury was induced by topical application of ferric chloride on a mesenteric arteriole, which provoked the generation of free radicals leading to the endothelial disruption.[23] The diameter and shear rate of studied arterioles were 118.0 plus or minus 13.1 μm and 1362 plus or minus 219 s^{-1} (mean ± SD, n = 16) for *Adamts13*$^{L/L}$ mice, 122.8 plus or minus 11.1 μm and 1394 plus or minus 136 s^{-1} (n = 16) for *Adamts13*$^{S/S}$ mice, and 115.6 plus or minus 10.8 μm and 1405 plus or minus 225 s^{-1} (n = 12) for *Adamts13*$^{-/-}$ mice and not significantly different among the groups. Both time to first thrombus (Figure 4A) and occlusion time (Figure 4B) after injury in *Adamts13*$^{-/-}$ mice (time to first thrombus = 5.1 ± 1.9 minutes, occlusion time = 9.2 ± 1.6 minutes; mean ± SD) were significantly decreased compared with *Adamts13*$^{L/L}$ mice (time to first thrombus = 7.8 ± 1.3 minutes, occlusion time = 15.3 ± 3.6 minutes), indicating that ADAMTS13 contributes to down-regulation of thrombogenesis at the site of arteriolar injury in 129/Sv mice. In the case of *Adamts13*$^{S/S}$ mice, time to first thrombus after injury (7.6 ± 1.2 minutes) was not different from *Adamts13*$^{L/L}$ mice. However, the initial thrombi grew rapidly to occlusive size in *Adamts13*$^{S/S}$ mice and occlusion time was significantly shorter in *Adamts13*$^{S/S}$ mice (12.5 ± 1.9 minutes) compared with *Adamts13*$^{L/L}$ mice (Figure 4B). These results suggest that the distal C-terminally truncated form of mouse ADAMTS13 is less active in down-regulating thrombus growth in vivo compared with full-length ADAMTS13.

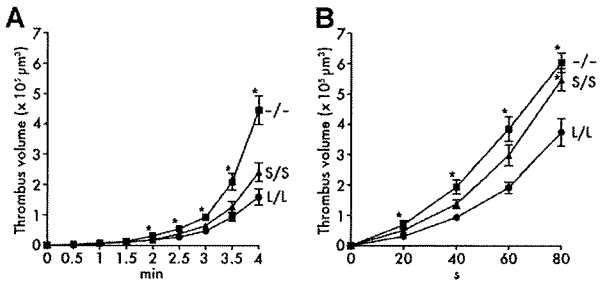

Figure 3. In vitro thrombogenesis on collagen surface under flow. (A) Thrombus formation at 1000 s^{-1}. Whole blood from *Adamts13*$^{L/L}$, *Adamts13*$^{S/S}$, or *Adamts13*$^{-/-}$ mice containing mepacrine-labeled platelets was perfused over an acid-insoluble type I collagen–coated surface at a wall shear rate of 1000 s^{-1}. The cumulative thrombus volume, analyzed using a multidimensional imaging system, was measured every 0.5 minutes until 4 minutes. Data are the mean ± SEM of 25 mice for each genotype. (B) Thrombus formation at 5000 s^{-1}. Whole-blood samples from indicated mice were perfused over an acid-insoluble type I collagen–coated surface at a wall shear rate of 5000 s^{-1}. The cumulative thrombus volume was measured every 20 seconds until 80 seconds. Blood from 2 mice was pooled and used for experiments. Data are the mean ± SEM of 15 samples for each genotype. *$P < .05$ in comparison with *Adamts13*$^{L/L}$ mice.

To elucidate the consequences of the lack of the distal C-terminal domains in ADAMTS13 on systemic thrombosis, we performed collagen plus epinephrine infusion model experiments. In this model, widespread intravascular thrombosis was induced by intravenous infusion of collagen fibrils in combination with epinephrine, and the incorporation of platelets into thrombi was monitored by the reduction in circulating platelet counts.[29] Consistent with our previous observation,[17] platelet counts after the infusion were significantly lower in *Adamts13*$^{-/-}$ mice

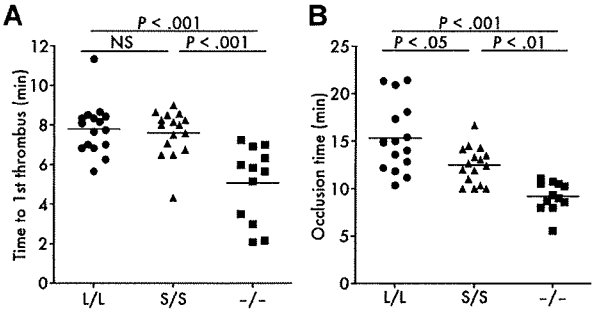

Figure 4. In vivo thrombogenesis in ferric chloride–injured mesenteric arterioles. (A) Time to first thrombus formation. Calcein AM–labeled platelets representing approximately 2.5% of total platelets were observed in mesenteric arterioles of live mice after injury with 10% ferric chloride. The time required for formation of a thrombus more than 30 μm was measured. (B) Occlusion time. The time required for a complete stop of blood flow was measured after injury with 10% ferric chloride. Symbols represent data from a single mouse. Bars represent the mean values of groups (n = 16 for *Adamts13*$^{L/L}$ mice, n = 16 for *Adamts13*$^{S/S}$ mice, and n = 12 for *Adamts13*$^{-/-}$ mice).

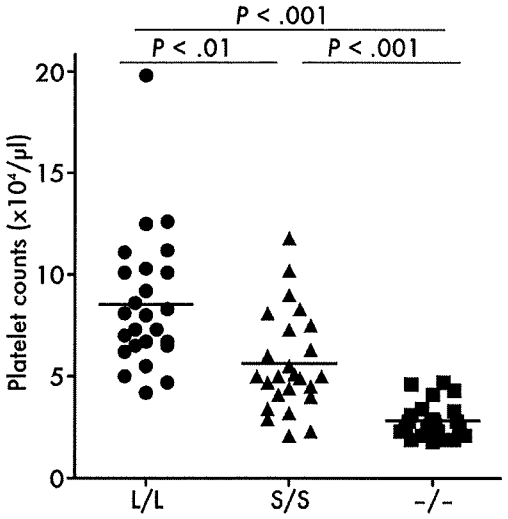

Figure 5. Platelet counts after collagen plus epinephrine infusion. Mice were injected with 600 ng/g collagen plus 60 ng/g epinephrine via tail vein and platelet counts were measured 5 minutes after injection. Symbols represent platelet counts from a single mouse. Bars represent the mean values of 25 mice in each group. Platelet counts of untreated mice were not different among the groups.

($28 \pm 8 \times 10^9$/L, mean ± SD) than in *Adamts13*$^{L/L}$ mice ($85 \pm 33 \times 10^9$/L), suggesting that ADAMTS13 contributes to inhibition of platelet aggregation in this experimental system (Figure 5). Platelet counts after the infusion in *Adamts13*$^{S/S}$ mice ($56 \pm 24 \times 10^9$/L) were significantly higher than in *Adamts13*$^{-/-}$ mice and lower than in *Adamts13*$^{L/L}$ mice (Figure 5), whereas platelet counts of untreated mice were not different among the groups (*Adamts13*$^{L/L}$, $666 \pm 44 \times 10^9$/L; *Adamts13*$^{S/S}$, $770 \pm 65 \times 10^9$/L; *Adamts13*$^{-/-}$, $710 \pm 49 \times 10^9$/L, mean ± SD of 4 mice). These findings complement accelerated thrombus growth in *Adamts13*$^{S/S}$ mice compared with *Adamts13*$^{L/L}$ mice, indicating that the distal C-terminally truncated form of mouse ADAMTS13 has significantly reduced activity in vivo.

Discussion

It is now evident that genetic background is an important phenotypic determinant in mutant mice with hemostatic defects. For instance, mice carrying the factor V Leiden (R504Q) mutation have shown increased perinatal thrombotic mortality on the mixed 129/Sv and C57BL/6J background relative to C57BL/6J background.[30] Similar effects of genetic backgrounds on phenotypes have been observed in other mutants such as the thrombomodulin G404P-mutant mice,[31] the fibrinogen-deficient mice,[32] and the tissue factor–deficient mice.[33] In ADAMTS13-deficient mice, genetic backgrounds have also been shown to significantly affect their thrombotic phenotypes.[34] Thus, phenotypes of ADAMTS13 mutant mice should be compared with control mice on the appropriate and uniform strain background. We have previously demonstrated that ADAMTS13 deficiency in mice results in a prothrombotic state with accumulation of UL-VWF multimers on 129/Sv background.[17] Therefore in this study, we applied a spontaneous mutation in the *Adamts13* gene of C57BL/6 mice onto 129/Sv mice by 10-generation backcrossing, and obtained the congenic mice that were expected to have 99.9% 129/Sv genome and primarily expressed the distal C-terminally truncated ADAMTS13. Then, we compared their phenotypes with positive and negative control animals: the wild-type 129/Sv mice and the 129/Sv-background ADAMTS13-deficient mice. By this approach, we minimized the background effects and defined the significance of the distal C-terminal domains of ADAMTS13 in mice.

Plasma of the congenic mice exhibited higher cleaving activity against GST-mVWF73-H and FRETS-VWF73 compared with plasma of the wild-type mice. We previously observed that the recombinant distal C-terminally truncated mouse ADAMTS13 cleaves GST-mVWF73-H to a similar extent compared with the full-length form.[14] The other group reported that the recombinant distal C-terminally truncated mouse ADAMTS13 is slightly less active in cleaving GST-mVWF73-H than the full-length form.[15] These findings suggest that the distal C-terminally truncated ADAMTS13 in mouse plasma has equivalent or slightly lower specific activity against VWF73-based substrates compared with the full-length ADAMTS13. Thus, the data in the present study imply that the distal C-terminally truncated ADAMTS13 is more abundant than the full-length form in circulating blood in 129/Sv mice. Preferential expression of the distal C-terminally truncated mouse ADAMTS13 has also been found in HeLa cells[14] and HEK 293T cells.[15] Unfortunately, because we have failed to determine the ADAMTS13 antigen levels in mouse plasma, it remains unclear whether the distal C-terminal truncation of ADAMTS13 actually increases plasma levels of the enzyme. Despite the congenic mice having higher in vitro ADAMTS13 activity in plasma, they showed prothrombotic phenotypes, suggesting the importance of the distal C-terminal domains in ADAMTS13 activity in vivo.

We reconfirmed that ADAMTS13 deficiency in 129/Sv mice allowed the accumulation of UL-VWF multimers in plasma (Figure 2), therefore, promising the essential contribution of ADAMTS13 on preventing the accumulation of UL-VWF multimers in 129/Sv mice. Under these situations, lack of the distal C-terminal domains of ADAMTS13 in 129/Sv mice did not increase plasma VWF multimer sizes (Figure 2), showing that the distal C-terminally truncated ADAMTS13 maintained the VWF-cleaving activity in vivo. Although the distal C-terminally truncated form of mouse ADAMTS13 was reported to show considerably lower activity than the full-length form for purified human VWF multimers under in vitro static conditions,[15] our results show that the distal C-terminal truncation of mouse ADAMTS13 allows retention of normal size distribution of plasma VWF multimers in vivo at least under steady state.

In the parallel-plate flow chamber experiments, ADAMTS13 deficiency in 129/Sv mice markedly enhanced thrombogenic responses (Figure 3), indicating that ADAMTS13 is critical for limiting platelet thrombus formation under whole blood flow conditions. In the same experimental conditions, the distal C-terminal truncation of ADAMTS13 in 129/Sv mice did not promote thrombogenesis at 1000 s^{-1} (Figure 3A) but significantly promoted thrombogenesis at 5000 s^{-1} (Figure 3B). It is conceivable that the distal C-terminally truncated ADAMTS13 is active but not fully competent to cleave VWF within growing thrombus under flow. Because both the interaction of GPIbα-VWF and the cleavage of VWF by ADAMTS13 are facilitated by increasing fluid shear rate, the function of the distal C-terminal domains may become vital to down-regulate thrombogenesis under high shear conditions. Actually, similar results were obtained in the in vivo arteriolar injury model experiments (Figure 4). The distal C-terminal truncation of ADAMTS13 in 129/Sv mice did not affect the time to first thrombus formation in the arterioles where fluid shear rates were around 1500 s^{-1} (Figure 4A). However, when thrombus grew to a larger size, the arteriolar lumen was narrowed, which resulted in increase in shear rates.[23] Then, the distal C-terminal truncation of

ADAMTS13 significantly reduced the occlusion time compared with full-length ADAMTS13 (Figure 4B). Therefore, the distal C-terminal domains are important for ADAMTS13 to sufficiently down-regulate thrombogenesis under high shear rate in vivo as well as in vitro. After the induction of systemic platelet aggregation by challenge with a mixture of collagen and epinephrine, consumptive thrombocytopenia was also enhanced by the distal C-terminal truncation of ADAMTS13 in 129/Sv mice (Figure 5), supporting the idea that the distal C-terminal domains are required for optimal down-regulation of platelet aggregation in vivo. The complete deficiency of ADAMTS13 in 129/Sv significantly accelerated thrombus growth to injured vessel wall and systemic thrombi compared with 129/Sv mice with truncation of the distal C-terminal domains in ADAMTS13 (Figures 4,5). Therefore, we can conclude that the distal C-terminally truncated ADAMTS13 has significantly decreased activity in limiting thrombosis in vivo.

The binding of platelets to VWF is reported to accelerate the cleavage of VWF by ADAMTS13 under static[35] and flow[36] conditions in vitro. It has also been shown that ADAMTS13 can cleave platelet-bound VWF multimers[37] and limit thrombus formation through the cleavage of VWF at the surface of forming thrombi[28] in in vitro flow chamber systems. Therefore, in our experimental settings, ADAMTS13 attenuates thrombus growth, possibly through the cleavage of VWF multimers bound on the surface of platelet-rich thrombi under high shear rate. The distal C-terminal domains may be necessary for ADAMTS13 to efficiently recognize and cleave platelet-bound VWF multimers on a growing thrombus. Conceivably, the distal C-terminal domains may contribute to the interaction with unidentified ADAMTS13-binding cofactors localized on the surface of platelets or subendothelium, and this interaction may be necessary for ADAMTS13 to control VWF-mediated thrombus formation. However, we cannot rule out the possibility that the distal C-terminal domains of ADAMTS13 contribute to the prevention of thrombosis independent from the VWF-cleaving activity of ADAMTS13, nevertheless VWF has been suggested as the only relevant substrate for ADAMTS13[38] and functions of ADAMTS13 other than its VWF-cleaving activity have yet to be reported.

The distal C-terminally truncated ADAMTS13 is expressed in a lot of mouse strains including the BALB/c, C3H/He, C57BL/6, and DBA/2 strains as substitute for the full-length form.[14,15] Our present results suggest that thrombotic response in these strains would be increased, at least partially, by their incomplete ADAMTS13 activity. This should be taken into account when studying genetically modified mice with heterogeneous genetic background.

In summary, our results define the role of the distal C-terminal domains in ADAMTS13 in vivo. Deletion of the C-terminal 2 Tsp1 and 2 CUB domains permits normal size distribution of plasma VWF multimers under steady state, but exacerbates platelet thrombosis after thrombogenic stimulation in mice. Thus, the distal C-terminally truncated ADAMTS13 is not fully active in vivo. These distal C-terminal domains of ADAMTS13 may play a role in the efficient processing of VWF multimers during platelet thrombus growth, and thus their functions may become increasingly important when vascular damage is induced.

Acknowledgments

We thank Ms Miyuki Kuroi and Ms Yuko Nobe (National Cardiovascular Center Research Institute), and Ms Meghan Walsh (Immune Disease Institute) for technical assistance.

This work was supported in part by grants-in-aid from the Ministry of Health, Labor, and Welfare of Japan, Tokyo, Japan (T.M.); the Ministry of Education, Culture, Sports, Science, and Technology of Japan, Tokyo, Japan (F.B., K.K., and T.M.); the Japan Society for the Promotion of Science, Tokyo, Japan (K.K. and T.M.); and from the Program for Promotion of Fundamental Studies in Health Sciences of the National Institute of Biochemical Innovation of Japan, Ibaraki, Japan (T.M.); a Sponsored Research Agreement from Baxter Bioscience, Vienna, Austria (A.K.C. and D.D.W.) and a National Heart, Lung, and Blood Institute of the National Institutes of Health grant P01-HL066105 (D.D.W.).

Authorship

Contribution: F.B. designed research, performed experiments, analyzed data, and wrote the paper; A.K.C. performed experiments, contributed vital analytical tools, and analyzed the data; K.K. designed research, performed experiments, and wrote the paper; J.Y. performed experiments and analyzed data; S.M. and D.D.W. contributed vital analytical tools and interpreted the data; and T.M. designed research and wrote the paper.

Conflict-of-interest disclosure: The authors declare no competing financial interests.

Correspondence: Toshiyuki Miyata, National Cardiovascular Center Research Institute, 5-7-1 Fujishirodai, Suita, Osaka 565-8565, Japan; e-mail: miyata@ri.ncvc.go.jp.

References

1. Dong JF. Structural and functional correlation of ADAMTS13. Curr Opin Hematol. 2007;14:270-276.
2. Bergmeier W, Chauhan AK, Wagner DD. Glycoprotein Ibalpha and von Willebrand factor in primary platelet adhesion and thrombus formation: lessons from mutant mice. Thromb Haemost. 2008;99:264-270.
3. Tsai HM. Thrombotic thrombocytopenic purpura: a thrombotic disorder caused by ADAMTS13 deficiency. Hematol Oncol Clin North Am. 2007;21:609-632.
4. Zheng XL, Sadler JE. Pathogenesis of thrombotic microangiopathies. Annu Rev Pathol. 2008;3:249-277.
5. Desch KC, Motto DG. Thrombotic thrombocytopenic purpura in humans and mice. Arterioscler Thromb Vasc Biol. 2007;27:1901-1908.
6. Soejima K, Matsumoto M, Kokame K, et al. ADAMTS-13 cysteine-rich/spacer domains are functionally essential for von Willebrand factor cleavage. Blood. 2003;102:3232-3237.
7. Zheng X, Nishio K, Majerus EM, Sadler JE. Cleavage of von Willebrand factor requires the spacer domain of the metalloprotease ADAMTS13. J Biol Chem. 2003;278:30136-30141.
8. Ai J, Smith P, Wang S, Zhang P, Zheng XL. The proximal carboxyl-terminal domains of ADAMTS13 determine substrate specificity and are all required for cleavage of von Willebrand factor. J Biol Chem. 2005;280:29428-29434.
9. Majerus EM, Anderson PJ, Sadler JE. Binding of ADAMTS13 to von Willebrand factor. J Biol Chem. 2005;280:21773-21778.
10. Tao Z, Wang Y, Choi H, et al. Cleavage of ultra-large multimers of von Willebrand factor by C-terminal-truncated mutants of ADAMTS-13 under flow. Blood. 2005;106:141-143.
11. Tao Z, Peng Y, Nolasco L, et al. Recombinant CUB-1 domain polypeptide inhibits the cleavage of ULVWF strings by ADAMTS13 under flow conditions. Blood. 2005;106:4139-4145.
12. Gao W, Anderson PJ, Majerus EM, Tuley EA, Sadler JE. Exosite interactions contribute to tension-induced cleavage of von Willebrand factor by the antithrombotic ADAMTS13 metalloprotease. Proc Natl Acad Sci U S A. 2006;103:19099-19104.
13. Zhang P, Pan W, Rux AH, Sachais BS, Zheng XL. The cooperative activity between the carboxyl-terminal TSP1 repeats and the CUB domains of ADAMTS13 is crucial for recognition of von Willebrand factor under flow. Blood. 2007;110:1887-1894.

14. Banno F, Kaminaka K, Soejima K, Kokame K, Miyata T. Identification of strain-specific variants of mouse Adamts13 gene encoding von Willebrand factor-cleaving protease. J Biol Chem. 2004;279:30896-30903.
15. Zhou W, Bouhassira EE, Tsai HM. An IAP retrotransposon in the mouse ADAMTS13 gene creates ADAMTS13 variant proteins that are less effective in cleaving von Willebrand factor multimers. Blood. 2007;110:886-893.
16. Banno F, Miyata T. Biology of an antithrombotic factor-ADAMTS13. In: Tanaka K, Davie EW, eds. Recent Advances in Thrombosis and Hemostasis. Berlin, Germany: Springer; 2008:162-176.
17. Banno F, Kokame K, Okuda T, et al. Complete deficiency in ADAMTS13 is prothrombotic, but it alone is not sufficient to cause thrombotic thrombocytopenic purpura. Blood. 2006;107:3161-3166.
18. Miyata T, Kokame K, Banno F, Shin Y, Akiyama M. ADAMTS13 assays and ADAMTS13-deficient mice. Curr Opin Hematol. 2007;14:277-283.
19. Kokame K, Matsumoto M, Fujimura Y, Miyata T. VWF73, a region from D1596 to R1668 of von Willebrand factor, provides a minimal substrate for ADAMTS-13. Blood. 2004;103:607-612.
20. Kokame K, Nobe Y, Kokubo Y, Okayama A, Miyata T. FRETS-VWF73, a first fluorogenic substrate for ADAMTS13 assay. Br J Haematol. 2005;129:93-100.
21. Tsuji S, Sugimoto M, Miyata S, Kuwahara M, Kinoshita S, Yoshioka A. Real-time analysis of mural thrombus formation in various platelet aggregation disorders: distinct shear-dependent roles of platelet receptors and adhesive proteins under flow. Blood. 1999;94:968-975.
22. Chauhan AK, Motto DG, Lamb CB, et al. Systemic antithrombotic effects of ADAMTS13. J Exp Med. 2006;203:767-776.
23. Ni H, Denis CV, Subbarao S, et al. Persistence of platelet thrombus formation in arterioles of mice lacking both von Willebrand factor and fibrinogen. J Clin Invest. 2000;106:385-392.
24. Frenette PS, Moyna C, Hartwell DW, Lowe JB, Hynes RO, Wagner DD. Platelet-endothelial interactions in inflamed mesenteric venules. Blood. 1998;91:1318-1324.
25. DiMinno G, Silver MJ. Mouse antithrombotic assay: a simple method for the evaluation of antithrombotic agents in vivo. Potentiation of antithrombotic activity by ethyl alcohol. J Pharmacol Exp Ther. 1983;225:57-60.
26. Jackson SP. The growing complexity of platelet aggregation. Blood. 2007;109:5087-5095.
27. Konstantinides S, Ware J, Marchese P, Almus-Jacobs F, Loskutoff DJ, Ruggeri ZM. Distinct antithrombotic consequences of platelet glycoprotein Ibalpha and VI deficiency in a mouse model of arterial thrombosis. J Thromb Haemost. 2006;4:2014-2021.
28. Shida Y, Nishio K, Sugimoto M, et al. Functional imaging of shear-dependent activity of ADAMTS13 in regulating mural thrombus growth under whole blood flow conditions. Blood. 2008;111:1295-1298.
29. Smyth SS, Reis ED, Vaananen H, Zhang W, Coller BS. Variable protection of beta 3-integrin–deficient mice from thrombosis initiated by different mechanisms. Blood. 2001;98:1055-1062.
30. Cui J, Eitzman DT, Westrick RJ, et al. Spontaneous thrombosis in mice carrying the factor V Leiden mutation. Blood. 2000;96:4222-4226.
31. Weiler H, Lindner V, Kerlin B, et al. Characterization of a mouse model for thrombomodulin deficiency. Arterioscler Thromb Vasc Biol. 2001;21:1531-1537.
32. Suh TT, Holmback K, Jensen NJ, et al. Resolution of spontaneous bleeding events but failure of pregnancy in fibrinogen-deficient mice. Genes Dev. 1995;9:2020-2033.
33. Toomey JR, Kratzer KE, Lasky NM, Broze GJ Jr. Effect of tissue factor deficiency on mouse and tumor development. Proc Natl Acad Sci U S A. 1997;94:6922-6926.
34. Motto DG, Chauhan AK, Zhu G, et al. Shigatoxin triggers thrombotic thrombocytopenic purpura in genetically susceptible ADAMTS13-deficient mice. J Clin Invest. 2005;115:2752-2761.
35. Nishio K, Anderson PJ, Zheng XL, Sadler JE. Binding of platelet glycoprotein Ibalpha to von Willebrand factor domain A1 stimulates the cleavage of the adjacent domain A2 by ADAMTS13. Proc Natl Acad Sci U S A. 2004;101:10578-10583.
36. Shim K, Anderson PJ, Tuley EA, Wiswall E, Sadler JE. Platelet-VWF complexes are preferred substrates of ADAMTS13 under fluid shear stress. Blood. 2008;111:651-657.
37. Donadelli R, Orje JN, Capoferri C, Remuzzi G, Ruggeri ZM. Size regulation of von Willebrand factor-mediated platelet thrombi by ADAMTS13 in flowing blood. Blood. 2006;107:1943-1950.
38. Chauhan AK, Walsh MT, Zhu G, Ginsburg D, Wagner DD, Motto DG. The combined roles of ADAMTS13 and VWF in murine models of TTP, endotoxemia, and thrombosis. Blood. 2008;111:3452-3457.

blood

2009 113: 5039-5040
doi:10.1182/blood-2009-02-201749

ADAMTS13's tail tale

Karen Vanhoorelbeke, Hendrik B. Feys and Simon F. De Meyer

Blood (print ISSN 0006-4971, online ISSN 1528-0020), is published semimonthly by the American Society of Hematology, 1900 M St, NW, Suite 200, Washington DC 20036.

there would be reluctance to advocate long-term primary prophylaxis, this should certainly be offered at times of additional high risk, such as after surgery, immobility, or pregnancy.

Clinically, the issue of thrombophilia testing and management is more relevant in the setting of patients who have experienced an event already. If testing has been performed and high-risk thrombophilia has been identified, this should certainly be taken into account when deciding on extended anticoagulation, especially for spontaneous events. The issue of whether all patients with a DVT should be screened for high-risk thrombophilia is unresolved[7] but, for those with a spontaneous event at a young age and a positive family history, this should be considered. Definition of a positive family history is difficult, but the suggestion offered in this paper of more than 20% of relatives affected is not evidence-based and would be dependent on relatives being available for study.[8]

Any decision on whether to offer long-term anticoagulation will depend on the risk of bleeding while on anticoagulants as well as the thrombotic risk. This study reports a very low annual bleeding risk at 0.29% but with wide confidence intervals, because it is based on only 2 events. The authors speculate that this may be because the thrombophilic defect reduces the bleeding risk, and this observation certainly requires confirmation. Alternative explanations are the young age of the cohort, the fact that the patients are cared for by expert centers, and the small number of events.

Conflict-of-interest disclosure: The author declares no competing financial interests. ■

REFERENCES

1. Egeberg O. Inherited antithrombin deficiency causing thrombophilia. Thromb Diath Haemorrh. 1965;13:516-530.
2. Raffini L. Thrombophilia in children: Who to test, how, when and why? Hematology Am Soc Hematology Educ Program. 2008;2008:228-235.
3. Lijfering WM, Brouwer J-LP, Veeger NJGM, et al. Selective testing for thrombophilia in patients with first venous thrombosis: results from a retrospective family cohort study on absolute thrombotic risk for currently known thrombophilic defects in 2479 relatives. Blood. 2009;113:5314-5322.
4. Lijfering WM, Mudler R, ten Kate MK, et al. Clinical relevance of decreased protein S levels: results from a retrospective family cohort involving 1143 relatives. Blood. 2009;113:1225-1230.
5. Simpson EL, Stevenson MD, Rawdin A, et al. Thrombophilia testing in people with venous thromboembolism: systematic review and cost effectiveness analysis. Health Technology Assessment. 2009;13:1-91.
6. Prandoni P, Lensing AWA, Cogo A, et al. The long term clinical course of acute deep vein thrombosis. Ann Intern Med. 1996;125:1-7.
7. Cohn D, Vansenne F, de Borgie C, et al. Thrombophilia testing for prevention of recurrent venous thromboembolism. Cochrane Database of Systematic Reviews. 2009;1. Art. No.: CD007069. DOI: 10.1002/14651858.CD007069.pub2
8. Cosmi B, Legnani C, Bernardi F, et al. Role of family history in identifying women with thrombophilia and higher risk of venous thromboembolism during oral contraception. Arch Intern Med. 2003;163:1105-1109.

● ● ● THROMBOSIS & HEMOSTASIS

Comment on Banno et al, page 5323

ADAMTS13's tail tale

Karen Vanhoorelbeke, Hendrik B. Feys, and Simon F. De Meyer KATHOLIEKE UNIVERSITEIT LEUVEN, CAMPUS KORTRIJK

In mice, a long form and a short form of the VWF-cleaving protease ADAMTS13 have been identified, the latter lacking the 4 distal carboxyl-terminal domains. While these are not strictly required for regulating normal size distribution of VWF multimers, in this issue of *Blood*, Banno and colleagues reveal the role of these domains in down-regulating thrombogenesis in vivo.

Since the discovery of ADAMTS13 as a metalloprotease with a multi-domain structure, numerous studies have attempted to shed light on the specific roles of each of the ADAMTS13 domains in digesting large von Willebrand factor (VWF) multimers into smaller, less reactive ones. ADAMTS13 is composed of a signal peptide, propeptide, metalloprotease domain, central TSR (thrombospondin type 1 repeat), Cys-rich region, spacer domain, 7 additional TSRs, and 2 CUB domains. The active site of this enzyme is situated in the metalloprotease domain while the spacer domain plays a crucial role in substrate binding by interacting with a VWF exosite located at the C-terminus of the A2 domain. The exact physiologic significance of the carboxyl-terminal TSRs and the 2 CUB domains still remains unclear, in particular due to the use of different types of in vitro tests, often performed under nonphysiological conditions.

To unravel the in vivo role of the carboxyl-terminal domains of ADAMTS13, Banno and coworkers elegantly take advantage of the presence of 2 kinds of *Adamts13* genes in laboratory mouse strains.[1] The 129/Sv strain has the *Adamts13* gene encoding full-length ADAMTS13 while several other strains, including C57BL/6, harbor an *Adamts13* gene that expresses a truncated form of the enzyme, lacking the 2 C-terminal TSRs and CUB domains due to the insertion of an intracisternal A-particle retrotransposon. By introgressing the C57BL/6-*Adamts13* gene onto the 129/Sv genetic background, the authors generate congenic mice that had the distal C-terminally truncated ADAMTS13 on a 129/Sv genetic background ($Adamts13^{S/S}$) and use wild-type mice that have full-length ADAMTS13 ($Adamts13^{L/L}$) and $ADAMTS13^{-/-}$ mice on the same 129/Sv genetic background for comparison.

The most obvious role of ADAMTS13 is to regulate VWF multimer size. Indeed, ADAMTS13 digests unusually large VWF multimers into smaller less thrombogenic forms,[2] hence preventing the spontaneous intravascular platelet aggregation seen in patients with ADAMTS13 deficiency. Interestingly, Banno et al showed that both $Adamts13^{L/L}$ and $Adamts13^{S/S}$ mice do not have ultra large VWF multimers in their plasma, implying that the C-terminal domains are not strictly needed for maintaining normal VWF size. Consequently, the 2 C-terminal TSRS and CUB domains are not essential for the removal of ultralarge VWF multimers from the plasma.

Following VWF size regulation, a fascinating role of ADAMTS13 in attenuating thrombus growth has been described, possibly by cleaving VWF multimers that are peripheral to or incorporated in platelet rich thrombi.[3] In this study, Banno et al used the congenic mice to demonstrate that the 2 C-terminal TSRs and CUB domains play a role in the down-regulation of thrombogenesis under high shear conditions. Both in vitro flow chamber experiments at high shear rates and in vivo thrombosis models show that blood from $Adamts13^{S/S}$ mice is more thrombogenic. This is evidenced by accelerated thrombus formation and decreased time to occlusion respectively when compared with blood from $Adamts13^{L/L}$ mice. Whether this would

translate into an increased risk of thrombosis in patients having comparable truncated forms of ADAMTS13 remains elusive.

In this article, Banno et al provide the first in vivo insights on the physiological significance of the distal carboxyl-terminal domains of ADAMTS13. The exact mechanism of thrombus size attenuation by ADAMTS13 and, in particular, the specific involvement of the carboxyl-terminal domains still remains to be determined. Does ADAMTS13 digest VWF multimers on the surface of the platelet thrombus or is thrombus size attenuation by ADAMTS13 independent of its VWF-cleaving activity? In this context, it is certainly intriguing that the mechanism of VWF size regulation by ADAMTS13 might be different from that of VWF processing during thrombus growth. Clearly, these new findings provide another impetus in the quest to understand the structure-function relationship of ADAMTS13. Obviously, this is not the end of the tale.

Conflict-of-interest disclosure: The authors declare no competing financial interests. ■

REFERENCES

1. Banno F, Chauhan A, Kokame K, et al. The distal carboxyl-terminal domains of ADAMTS13 are required for regulation of in vivo thrombus formation. Blood. 2009;113: 5323-5329.

2. Dong JF, Moake JL, Nolasco L, et al. ADAMTS-13 rapidly cleaves newly secreted ultralarge von Willebrand factor multimers on the endothelial surface under flowing conditions. Blood. 2002;100:4033-4039.

3. Chauhan AK, Motto DG, Lamb CB, et al. Systemic antithrombotic effects of ADAMTS13. J Exp Med. 2006; 203:767-776.

● ● ● TRANSPLANTATION

Comment on Kamei et al, page 5041

Scanning for the origins of mHags

John A. Hansen FRED HUTCHINSON CANCER RESEARCH CENTER

In this issue of *Blood*, Kamei and colleagues introduce an innovative approach for identifying the genes that encode novel T cell–defined human minor histocompatibility antigens (mHags). In this significant methodologic advance, they demonstrate how the rich human genetic variation data generated for the International Human HapMap Project, together with the available HapMap B-lymphoblastoid cell lines that have undergone extensive genome-wide sequencing, can be used to identify the functional genetic variants responsible for the cellular peptides recognized by selected T-cell clones.

Human minor histocompatibility antigens (mHags) have been recognized as barriers to successful hematopoietic cell transplantation (HCT) from normal donors for more than 30 years.[1] Success following HCT is ultimately determined by the ability to achieve sustained engraftment, eradication of abnormal or malignant host cells, and control of graft-versus-host disease (GVHD). Each of these clinical end points is influenced by the nature and extent of the genetic disparity between donor and recipient. Graft rejection and GVHD are immune-mediated reactions induced by histocompatibility differences between donor and recipient. GVHD occurs when immune-competent donor T cells are transplanted to an immune-compromised host, and the incompatibility between donor and recipient is sufficient to induce T-cell activation.[2] The histocompatibility differences responsible for these T-cell responses are encoded by polymorphic genes located throughout the genome. T-cell recognition of these differences can occur only when the variant peptide in a recipient is foreign to the donor and is appropriately processed and presented at the cell surface by the HLA alleles of the recipient. Polymorphic peptides fulfilling these requirements are called mHags.[1,3]

Although severe GVHD has an adverse effect on morbidity and mortality, occurrence of GVHD is also associated with lower relapse rates, demonstrating that host reactivity of donor T cells can also mediate a significant graft-versus-leukemia (GVL) effect and thereby directly contributes to the curative potential of allogeneic HCT for patients with hematologic malignancy. The GVL effect has become an important model system for exploring new strategies aimed at improving the antitumor potential of T cell–based immunotherapy. These efforts have largely focused on understanding the mechanisms of GVL and the identification of the molecules that could be the potential targets for T-cell immunotherapy.[4,5] Improved techniques for cloning mHag-specific T cells and eluting candidate peptides from major histocompatibility complex molecules in the late 1980s made possible the initial identification of individual mHags. However, the process was difficult, and progress in expanding the library of well-characterized mHags has been slow.

In this issue of *Blood*, Kamei et al introduce a novel approach for identifying T cell–defined mHag loci using publically available resources generated by the International HapMap Project and including the B-lymphoblastoid cell lines that were the source of DNA sequenced for the HapMap project and the resulting large dataset of sequence-based genotypes.[6-8] These cell lines are publicly available, and once they have been transduced with the appropriate HLA restriction element, they can be tested as targets to determine whether they contain the DNA sequence necessary to encode specific T cell–defined peptides. Mapping of the gene encoding the mHag is accomplished by combining the results of immune-based functional assays with a whole genome association analysis by scanning the known sequence polymorphisms (SNPs) in the vast HapMap database, which currently consists of more than 3 million genetic markers expressed by these reference cell lines. The power and resolution of genetic mapping obtainable with this resource will continue to expand in the future as the numbers of new reference samples sequenced increases, and the racial diversity of the reference panel is broadened. The approach described here by Kamei et al should contribute substantially to the development of a more comprehensive and efficient characterization of mHags. This method may also prove useful for the genetic mapping of other genetic traits.

Conflict-of-interest disclosure: The author declares no competing financial interests. ■

REFERENCES

1. Snell GD, Dausset J, Nathenson S. Histocompatibility. New York, NY: Academic Press; 1976.

2. Elkins WL. Cellular immunology and the pathogenesis of graft versus host reactions (review). Prog Allergy. 1971; 15:78-187.

3. Perreault C, Décary F, Brochu S, et al. Minor histocompatibility antigens. Blood. 1990;76:1269-1280.

4. Bleakley M, Riddell SR. Molecules and mechanisms of the graft-versus-leukaemia effect. Nat Rev Cancer. 2004;4:371-380.

5. Spierings E, Goulmy E. Expanding the immunotherapeutic potential of minor histocompatibility antigens. J Clin Invest. 2005;115:3397-3400.

6. Kamei M, Nannya Y, Torikai H, et al. HapMap scanning of novel human minor histocompatibility antigens. Blood. 2009;113:5041-5048.

7. The International HapMap Consortium. The International HapMap Project. Nature. 2003;426:789-796.

8. Frazer KA, Ballinger DG, Cox DR, et al. A second generation human haplotype map of over 3.1 million SNPs. Nature. 2007;449:851-861.

Brief report

ADAMTS13 gene deletion aggravates ischemic brain damage: a possible neuroprotective role of ADAMTS13 by ameliorating postischemic hypoperfusion

*Masayuki Fujioka,[1-3] *Kazuhide Hayakawa,[2] Kenichi Mishima,[2] Ai Kunizawa,[3] Keiichi Irie,[2] Sei Higuchi,[2] Takafumi Nakano,[2] Carl Muroi,[3] Hidetada Fukushima,[1] Mitsuhiko Sugimoto,[4] Fumiaki Banno,[5] Koichi Kokame,[5] Toshiyuki Miyata,[5] Michihiro Fujiwara,[2] Kazuo Okuchi,[1] and Kenji Nishio[1]

[1]Department of Emergency and Critical Care Medicine, Nara Medical University, Nara, Japan; [2]Department of Neuropharmacology, Faculty of Pharmaceutical Sciences, Fukuoka University, Fukuoka, Japan; [3]Stroke Center, Helios General Hosp Aue, Dresden University of Technology, Saxony, Germany; [4]Department of Regulatory Medicine for Thrombosis, Nara Medical University, Nara, Japan; and [5]Research Institute, National Cardiovascular Center, Suita, Japan

Reperfusion after brain ischemia causes thrombus formation and microcirculatory disturbances, which are dependent on the platelet glycoprotein Ib–von Willebrand factor (VWF) axis. Because ADAMTS13 cleaves VWF and limits platelet-dependent thrombus growth, ADAMTS13 may ameliorate ischemic brain damage in acute stroke. We investigated the effects of ADAMTS13 on ischemia-reperfusion injury using a 30-minute middle cerebral artery occlusion model in *Adamts13*$^{-/-}$ and wild-type mice. After reperfusion for 0.5 hours, the regional cerebral blood flow in the ischemic cortex was decreased markedly in *Adamts13*$^{-/-}$ mice compared with wild-type mice ($P < .05$), which also resulted in a larger infarct volume after 24 hours for *Adamts13*$^{-/-}$ compared with wild-type mice ($P < .01$). Thus, *Adamts13* gene deletion aggravated ischemic brain damage, suggesting that ADAMTS13 may protect the brain from ischemia by regulating VWF-platelet interactions after reperfusion. These results indicate that ADAMTS13 may be a useful therapeutic agent for stroke. (Blood. 2010; 115:1650-1653)

Introduction

von Willebrand factor (VWF) is a large multimeric protein that plays a key role in thrombus formation by tethering platelets at sites of vascular injury.[1] Smaller VWF multimers are less active, and the potent thrombogenic activity of ultra-large VWF (ULVWF) secreted from endothelium is regulated in vivo through cleavage by ADAMTS13.[2,3] The importance of this mechanism for normal hemostasis is supported by evidence that patients with deficiency of ADAMTS13 function, diagnosed with thrombotic thrombocytopenic purpura, have ULVWF in circulating blood and VWF-dependent microvascular thrombosis.[2] Recently, we demonstrated that ADAMTS13 cleaves VWF on the surface of platelet thrombi in a shear force–dependent manner, which limits thrombus growth in vitro.[4] These data suggest that ADAMTS13 is a key molecule that maintains a physiologic balance between hemostasis and thrombosis through regulation of VWF function in vivo.

ADAMTS13 function is crucial for preventing thrombosis in the cerebral microvasculature, as indicated by the occurrence of neurologic deficits in thrombotic thrombocytopenic purpura, but the role of ADMTS13 in the pathogenesis of reperfusion injury after arterial thrombosis has not been established. To address this issue, we investigated the role of ADAMTS13 in a transient middle cerebral arterial occlusion (MCAO) model of ischemia-reperfusion injury in the mouse brain[5] using *Adamts*$^{-/-}$ mice.[6]

Because brain ischemia-reperfusion injury is dependent on the platelet glycoprotein Ib–VWF axis[7] and platelet thrombosis adversely affects the postischemic cerebral microcirculation[8-11] leading to secondary brain damage,[10] ADAMTS13 may reduce platelet thrombus growth and thereby ameliorate ischemic brain injury by improving the postischemic no-reflow phenomenon.[12] Here we demonstrate that *Adamts13* gene deletion aggravates postischemic cerebral blood reflow, resulting in larger infarct volume. This result suggests that ADAMTS13 may indeed suppress excessive platelet thrombus growth in vivo.

Methods

The effect of *Adamts13* gene deletion on brain ischemia was studied using male *Adamts13*$^{-/-}$ (−/−) mice and wild-type (+/+) mice generated by our study group.[6] We used male mice only to obtain consistent results because female mice are known to be more resistant to stroke. The experimenters were blinded to the genotype of each animal until all studies had been finished. This study was approved by the institutional ethics committee of Fukuoka University.

Transient MCAO

Focal cerebral ischemia (MCAO by intraluminal thread) was induced in *Adamts13*$^{-/-}$ and wild-type mice as previously described.[5,13,14] Preliminary experiments using 1-hour MCAO gave excessively high mortality of 4 of 5 for one group and 1 of 4 for another. Therefore, we reduced the time of MCAO to 30 minutes. Body temperature was maintained at 36.5°C to 37.0°C during surgery. The success of the left MCAO was confirmed according to the following criteria: (1) regional cerebral blood flow (rCBF)

Submitted June 29, 2009; accepted October 20, 2009. Prepublished online as *Blood* First Edition paper, November 13, 2009; DOI 10.1182/blood-2009-06-230110.

*M. Fujioka and K.H. contributed equally to this study.

This study was presented in part at the 50th Annual Meeting of the American Society of Hematology, San Francisco, CA, December 6-9, 2008.

An Inside *Blood* analysis of this article appears at the front of this issue.

The publication costs of this article were defrayed in part by page charge payment. Therefore, and solely to indicate this fact, this article is hereby marked "advertisement" in accordance with 18 USC section 1734.

in the left cerebral cortex at the thread insertion less than 20% of pre-MCAO rCBF; and (2) consistent presence of significant ischemic neurologic symptoms of the left cerebral hemisphere, including right forepaw paralysis and right circling behavior during 30-minute MCAO.

rCBF

The rCBF was measured by LASER Doppler flowmetry (LDF; ALF21, Advance Co) as previously described.[5] The LDF probe was placed in the left cerebral cortex stereotaxically. The rCBF was monitored in all animals during the period between 30 minutes before MCAO and immediately after reperfusion.

Cerebral infarct volume and histology 24 hours after MCAO

The brains were sectioned coronally (four 2-mm-thick slices) according to a mouse brain matrix 24 hours after MCAO or sham operation. The infarct area was measured using an image-analysis system (National Institutes of Health Image software, Version 1.63) in each slice stained with 2,3,5 triphenyltetrazolium chloride, and the infarct volume was calculated.[5,13] Paraffin-embedded brains were stained with phosphotungstic acid hematoxylin (PTAH) to demonstrate fibrin in thrombi or incubated with anti-VWF antibody (sc-8068; Santa Cruz Biotechnology), followed by a standard avidin-biotin-peroxidase complex technique to demonstrate VWF in thrombi.

Neurologic assessment

Neurologic deficit was assessed at 24 hours after MCAO using a neurologic score as previously described,[13] and the survival rates were also measured at 24 hours after MCAO.

Statistical analysis

Data are mean plus or minus SEM. For multiple pairwise comparisons, 2-way analysis of variance followed by Scheffé test was performed. When only 2 groups were compared, Student *t* test was used. Probability values less than .05 were considered to be of statistical significance.

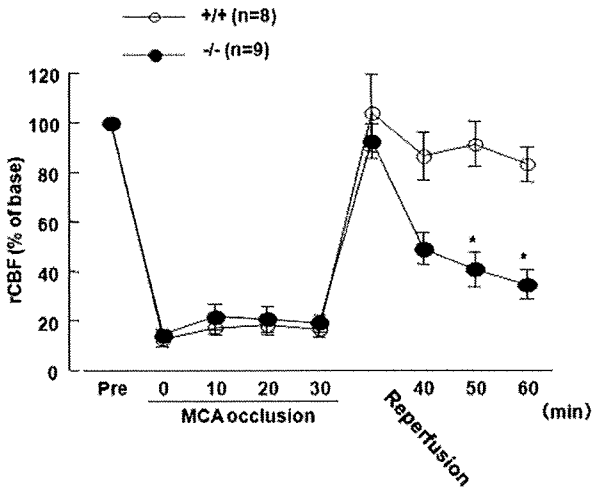

Figure 1. Effect of *Adamts13* gene deletion on rCBF in mice of 30-minute MCAO model. Male *Adamts13*$^{-/-}$ (−/−) mice and wild-type (+/+) mice in an SV129-genetic background were used to study the effect of ADAMTS13 deficiency on brain ischemia: −/− (n = 25) and +/+ (n = 25) mice (8-10 weeks of age, 20-23 g of body weight). The focal cerebral ischemia (30-minute MCAO by intraluminal thread) was induced in the −/− (n = 20) and +/+ (n = 20) mice as previously described (sham surgery in −/−, n = 5; and +/+, n = 5). This study was approved by the institutional ethics committee at Nara Medical University. The rCBF was measured by LDF (ALF21; Advance Co). The rCBF was recorded over time (immediately before and after MCAO; 10, 20, and 30 minutes after MCAO; immediately after reperfusion; and 10, 20, and 30 minutes after reperfusion). The rCBFs during occlusion and reperfusion were expressed as a percentage of the baseline LDF value. The rCBF decreased to less than 20% of the baseline value during 30 minutes of MCAO and returned to the baseline immediately after reperfusion in both −/− and WT mice. The rCBF in −/− mice, however, progressively decreased more markedly compared with that in +/+ after reperfusion (percentage rCBF: −/−, n = 9, vs +/+, n = 8, at 20 and 30 minutes after reperfusion; 40.8 ± 7.1 vs 91.4 ± 9.1, and 34.6 ± 5.8 vs 83.2 ± 6.8, respectively). *$P < .05$ vs WT, Scheffé test after 2-way repeated-measures analysis of variance ($F(8,134) = 6.668$, $P < .01$). Values are mean ± SEM.

Results and discussion

The rCBF decreased to less than 20% of the baseline value during 30-minute MCAO and returned to baseline immediately after reperfusion in both *Adamts13*$^{-/-}$ and wild-type mice. However, during the subsequent 30 minutes, the rCBF for both groups decreased, suggesting that ischemia-reperfusion had induced thrombosis. The rCBF for *Adamts13*$^{-/-}$ mice progressively decreased compared with wild-type mice (significantly decreased at 20 and 30 minutes after reperfusion, $P < .05$, Scheffé test, Figure 1).

The survival rates of the *Adamts13*$^{-/-}$ and wild-type mice did not differ (17 of 20 vs 16 of 20, respectively). However, *Adamts13*$^{-/-}$ mice had larger brain infarctions compared with wild-type mice 24 hours after MCAO ($P < .01$; Figure 2A), which is reflected by a difference in neurologic score assessing left hemisphere function (Figure 2B). Histologic and immunohistochemical examinations revealed that more thrombi containing fibrin and VWF were observed in *Adamts13*$^{-/-}$ mice (Figure 2C), which may contribute to the lowered rCBF and increased infarct volume in *Adamts13*$^{-/-}$ mice. These results indicate that *Adamts13* gene deletion aggravates ischemic brain damage.

Our results indicate that ADAMTS13 is crucial in vivo to protect the brain from ischemia-reperfusion injury by ameliorating postischemic hypoperfusion. The possible neuroprotective effect of ADAMTS13 may result from the cleavage of ULVWF secreted from endothelium activated by ischemia[3,15] and cleavage of VWF multimers on the surface of thrombi formed on the ischemic endothelial cells.[4] Without adequate ADAMTS13, progressive platelet thrombus growth may narrow the microvascular lumen, increasing fluid shear stress locally. Without negative feedback regulation by proteolysis of VWF, ischemia-reperfusion injury may cause a vicious cycle in which the VWF-platelet thrombosis and fluid shear stress enhance each other and contribute to the progressive deterioration of cerebral blood reflow, as observed in the *Adamts13*$^{-/-}$ mice. ADAMTS13 may, therefore, prevent microvascular occlusion under high shear stress and augment the cerebral blood flow after ischemia-reperfusion in vivo.

In addition to VWF-platelet thrombus formation,[10,11,16,17] microvascular plugging by activated leukocytes[18-20] can lead to no-reflow phenomena in brain ischemia.[11] Importantly, platelet-ULVWF strings support leukocyte tethering on the endothelium under high fluid-shear stress.[21,22] A recent study suggested that deficiency of ADAMTS13 can increase leukocyte adhesion on the vessels and extravasation.[23] Thus, ADAMTS13 deficiency may enhance the leukocyte activation in the ischemic cerebral vasculature after reperfusion and thereby aggravate ischemic brain damage. Indeed, *Adamts13*$^{-/-}$ mice accumulated more inflammatory cells in the brain tissue than wild-type mice after MCAO (Figure 2C), suggesting that ADAMTS13 may reduce inflammation as well as thrombosis associated with ischemia-reperfusion injury.

In conclusion, ADAMTS13 deficiency causes progressive decline of postischemic rCBF, with a resultant exacerbation of ischemic brain injury, suggesting an important role of ADAMTS13 in neuroprotection. The regulation of VWF-platelet interactions by supplementation with ADAMTS13 may ameliorate ischemia-reperfusion injury of the brain. Because ADAMTS13 tends to

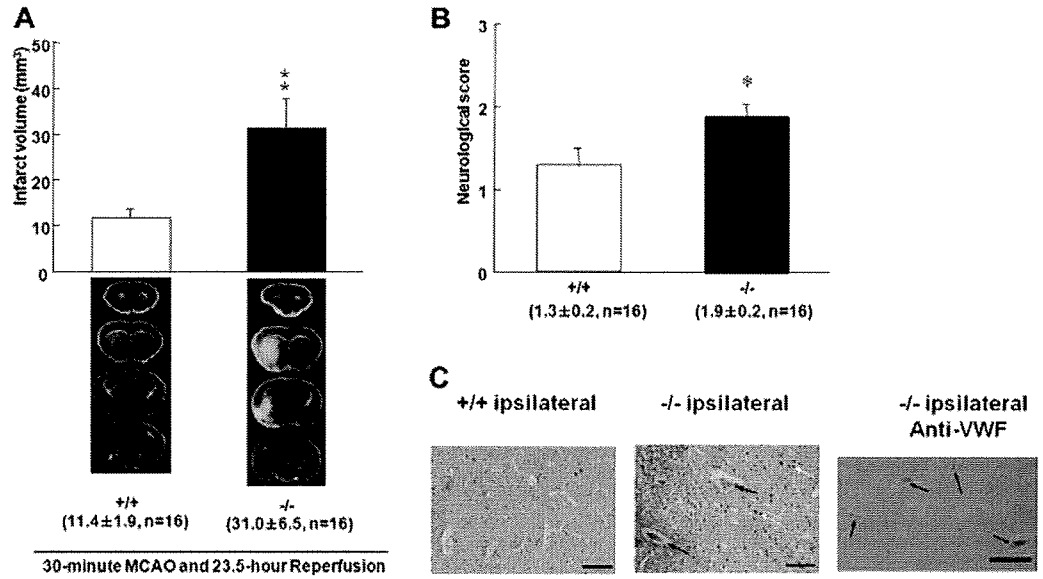

Figure 2. Effect of *Adamts13* gene deletion on brain infarct in mice after 30-minute MCAO. (A) These are coronal sections through the brain in both groups stained with 2,3,5 triphenyltetrazolium chloride. Red areas represent vital brain tissue, and white areas represent cerebral infarction. *Adamts13*$^{-/-}$ (−/−) mice had significantly larger volume of brain infarct compared with wild-type (+/+) mice after 23.5-hour reperfusion after 30-minute MCAO (−/−, n = 16, vs +/+, n = 16, $^{**}P < .01$, Student *t* test). Values are mean ± SEM (mm^3). The average infarct volume was 31.0 ± 6.5 mm^3 for ADAMTS13 $^{-/-}$ mice and 11.4 ± 1.9 mm^3 for +/+ mice. The survival rates of the −/− and +/+ mice did not differ (17 of 20 vs 16 of 20, respectively). No ischemic change was observed in the brain of −/− and +/+ mice after sham operation. (B) Neurologic score was measured 24 hours after MCAO. Neurologic scores were measured from the point according to the neurologic findings as follows: 0 indicates normal motor function; 1, flexion of torso and of contralateral forelimb on lifting of the animal by the tail; 2, circling to the ipsilateral side but normal posture at rest; 3, circling to the ipsilateral side; 4, rolling to the ipsilateral side; and 5, leaning to the ipsilateral side at rest (no spontaneous motor activity). $^{*}P < .05$. (C) Representative PTAH-stained sections of infarct area for wild-type (+/+) and *Adamts13*$^{-/-}$ (−/−) mice. There were more thrombi and inflammatory cells in the lesions of *Adamts13*$^{-/-}$ mice compared with +/+ mice (black arrows represent thrombus; white arrow, inflammatory cells infiltration). The area comparable with PTAH staining for −/− mice was immunostained using anti-VWF antibody. VWF is detected in thrombi as brown staining (−/− ipsilateral anti-VWF). Images were generated using an Olympus BH-2 microscope with an Olympus DP20-5 digital camera (original magnification ×200). Bar represents 40 μm.

dissolve excessive VWF-platelet thrombi with increasing efficiency as the flow path narrows, treatment of acute ischemic stroke with ADAMTS13 might have a relatively low risk of hemorrhagic complications.

Note added in proof. After submission of our paper, the complementary paper by Zhao et al[24] appeared in *Blood*, which also demonstrated the important role of ADAMTS13 for brain reperfusion injury.

Acknowledgments

The authors thank Dr Kouko Tatsumi and Dr Takahiko Kasai at the Laboratory of the Department of Anatomy and Neuroscience, and Diagnostic Pathology, respectively, in Nara Medical University, for histologic assistance.

Authorship

Contribution: M. Fujioka and K.H. performed most of the animal experiments and prepared the manuscript; A.K., K.I., S.H., T.N., and C.M. helped to perform the animal experiments; H.F. and M.S. worked on the experimental design and data analysis; K.M., M. Fujiwara, K.O., and K.N. provided direction throughout the work, made the overall experimental design, and edited the manuscript; and F.B., K.K., and T.M. produced the ADAMTS13 gene-deleted mice.

Conflict-of-interest disclosure: The authors declare no competing financial interests.

Correspondence: Kenji Nishio, Department of Emergency and Critical Care Medicine, Nara Medical University, 840 Shijo-cho, Kashihara, Nara 634-8522, Japan; e-mail: knishio@naramed-u.ac.jp.

References

1. Ruggeri ZM. Von Willebrand factor, platelets and endothelial cell interactions. *J Thromb Haemost.* 2003;1(7):1335-1342.
2. Sadler JE. Von Willebrand factor, ADAMTS13, and thrombotic thrombocytopenic purpura. *Blood.* 2008;112(1):11-18.
3. Dong JF, Moake JL, Nolasco L, et al. ADAMTS-13 rapidly cleaves newly secreted ultralarge von Willebrand factor multimers on the endothelial surface under flowing conditions. *Blood.* 2002; 100(12):4033-4039.
4. Shida Y, Nishio K, Sugimoto M, et al. Functional imaging of shear-dependent activity of ADAMTS13 in regulating mural thrombus growth under whole blood flow conditions. *Blood.* 2008; 111(3):1295-1298.
5. Hayakawa K, Mishima K, Nozako M, et al. Delayed treatment with cannabidiol has a cerebroprotective action via a cannabinoid receptor-independent myeloperoxidase-inhibiting mechanism. *J Neurochem.* 2007;102(5):1488-1496.
6. Banno F, Kokame K, Okuda T, et al. Complete deficiency in ADAMTS13 is prothrombotic, but it alone is not sufficient to cause thrombotic thrombocytopenic purpura. *Blood.* 2006;107(8):3161-3166.
7. Kleinschnitz C, De Meyer SF, Schwarz T, et al. Deficiency of von Willebrand factor protects mice from ischemic stroke. *Blood.* 2009;113(15):3600-3603.
8. Stoll G, Kleinschnitz C, Nieswandt B. Molecular mechanisms of thrombus formation in ischemic stroke: novel insights and targets for treatment. *Blood.* 2008;112(9):3555-3562.
9. Kochanek PM, Dutka AJ, Kumaroo KK, Hallenbeck JM. Effects of prostacyclin, indomethacin, and heparin on cerebral blood flow and platelet adhesion after multifocal ischemia of canine brain. *Stroke.* 1988;19(6):693-699.

10. Lo EH, Dalkara T, Moskowitz MA. Mechanisms, challenges and opportunities in stroke. *Nat Rev Neurosci.* 2003;4(5):399-415.
11. del Zoppo GJ, Mabuchi T. Cerebral microvessel responses to focal ischemia. *J Cereb Blood Flow Metab.* 2003;23(8):879-894.
12. Ames A 3rd, Wright RL, Kowada M, Thurston JM, Majno G. Cerebral ischemia: II. the no-reflow phenomenon. *Am J Pathol.* 1968;52(2):437-453.
13. Hayakawa K, Mishima K, Nozako M, et al. Delayed treatment with minocycline ameliorates neurologic impairment through activated microglia expressing a high-mobility group box1-inhibiting mechanism. *Stroke.* 2008;39(3):951-958.
14. Limbourg FP, Huang Z, Plumier JC, et al. Rapid nontranscriptional activation of endothelial nitric oxide synthase mediates increased cerebral blood flow and stroke protection by corticosteroids. *J Clin Invest.* 2002;110(11):1729-1738.
15. Huang J, Roth R, Heuser JE, Sadler JE. Integrin alpha(v)beta(3) on human endothelial cells binds von Willebrand factor strings under fluid shear stress. *Blood.* 2009;113(7):1589-1597.
16. Kleinschnitz C, Stoll G, Bendszus M, et al. Targeting coagulation factor XII provides protection from pathological thrombosis in cerebral ischemia without interfering with hemostasis. *J Exp Med.* 2006;203(3):513-518.
17. Kleinschnitz C, Pozgajova M, Pham M, Bendszus M, Nieswandt B, Stoll G. Targeting platelets in acute experimental stroke: impact of glycoprotein Ib, VI, and IIb/IIIa blockade on infarct size, functional outcome, and intracranial bleeding. *Circulation.* 2007;115(17):2323-2330.
18. Ishikawa M, Cooper D, Arumugam TV, Zhang JH, Nanda A, Granger DN. Platelet-leukocyte-endothelial cell interactions after middle cerebral artery occlusion and reperfusion. *J Cereb Blood Flow Metab.* 2004;24(8):907-915.
19. Connolly ES Jr, Winfree CJ, Springer TA, et al. Cerebral protection in homozygous null ICAM-1 mice after middle cerebral artery occlusion: role of neutrophil adhesion in the pathogenesis of stroke. *J Clin Invest.* 1996;97(1):209-216.
20. Mori E, del Zoppo GJ, Chambers JD, Copeland BR, Arfors KE. Inhibition of polymorphonuclear leukocyte adherence suppresses no-reflow after focal cerebral ischemia in baboons. *Stroke.* 1992; 23(5):712-718.
21. Bernardo A, Ball C, Nolasco L, Choi H, Moake JL, Dong JF. Platelets adhered to endothelial cell-bound ultra-large von Willebrand factor strings support leukocyte tethering and rolling under high shear stress. *J Thromb Haemost.* 2005;3(3):562-570.
22. Pendu R, Terraube V, Christophe OD, et al. P-selectin glycoprotein ligand 1 and beta2-integrins cooperate in the adhesion of leukocytes to von Willebrand factor. *Blood.* 2006;108(12):3746-3752.
23. Chauhan AK, Kisucka J, Brill A, Walsh MT, Scheiflinger F, Wagner DD. ADAMTS13: a new link between thrombosis and inflammation. *J Exp Med.* 2008;205(9):2065-2074.
24. Zhao BQ, Chauhan AK, Canault M, et al. von Willebrand factor-cleaving protease ADAMTS13 reduces ischemic brain injury in experimental stroke. *Blood.* 2009;114(15):3329-3334.

Int J Hematol (2010) 91:30–35
DOI 10.1007/s12185-009-0477-0

The function of ADAMTS13 in thrombogenesis in vivo: insights from mutant mice

Fumiaki Banno · Anil K. Chauhan · Toshiyuki Miyata

Received: 31 August 2009 / Accepted: 16 December 2009 / Published online: 5 January 2010

Abstract Recently, two independent groups have established ADAMTS13-deficient mice using gene-targeting techniques. In humans, genetic or acquired deficiency in ADAMTS13 leads to a potentially fatal syndrome, thrombotic thrombocytopenic purpura (TTP). Surprisingly, ADAMTS13-deficient mice are viable with no apparent signs of TTP. However, these mouse models indicate that ADAMTS13 down-regulates platelet adhesion and aggregation in vivo, and ADAMTS13 deficiency can provide enhanced thrombus formation at the site of vascular lesions. In addition, ADAMTS13 by cleaving hyperactive ultra-large von Willebrand factor multimers not only down-regulates thrombosis but also inflammation. ADAMTS13-congenic mice that carry a truncated form of ADAMTS13 lacking the C-terminal domains have also been developed. Phenotypes of the congenic mice indicate the physiological significance of the C-terminal domains of ADAMTS13 in down-regulating thrombus growth. The studies mentioned here in different mouse models uncover the in vivo function of ADAMTS13 and strengthened the understanding of the mechanism of systemic disease TTP.

F. Banno · T. Miyata (✉)
National Cardiovascular Center Research Institute,
5-7-1 Fujishirodai, Suita, Osaka 565-8565, Japan
e-mail: miyata@ri.ncvc.go.jp

F. Banno
e-mail: banno@ri.ncvc.go.jp

A. K. Chauhan
Department of Internal Medicine,
University of Iowa Carver College of Medicine,
500 Newton Road, Iowa, IA 52242, USA
e-mail: anil-chauhan@uiowa.edu

Keywords ADAMTS13 · von Willebrand factor · ADAMTS13-deficient mice · ADAMTS13-congenic mice · Thrombosis · Inflammation

1 Introduction

ADAMTS13 is a plasma protease that cleaves von Willebrand factor (VWF) [1]. VWF is a large protein that circulates in blood as homomultimers of varied sizes. One of main functions of VWF is to mediate adhesion between platelets and between platelets and vascular subendothelium. Both types of adhesion are essential to maintain the balance between hemorrhage and thrombosis. The adhesive activity of VWF depends on its molecular sizes and, in particular, ultra-large VWF (UL-VWF) multimers exceeding 20,000 kDa can form high strength bonds with platelet GPIbα and induce excessive platelet aggregation under shear stress. UL-VWF multimers are normally cleaved by ADAMTS13 to smaller forms, thus restraining spontaneous platelet thrombus formation. The lack of ADAMTS13 activity allows UL-VWF multimers to persist in the circulation and leads to the development of thrombotic thrombocytopenic purpura (TTP) [1].

TTP is a serious systemic disease caused by excessive aggregation of platelets and VWF in small vessels of many organs. The accumulated platelet thrombi obstruct blood flow and cause consumptive thrombocytopenia, fragmentation of red blood cells with anemia, renal and cerebral failure, and fever. Without treatment, the mortality rate of affected patients exceeds 90%, but plasma exchange reduces the death rate to approximately 20%. The discovery of ADAMTS13 as VWF-cleaving protease increases our understanding of TTP pathophysiology. Congenital TTP (Upshaw-Schulman syndrome) is associated with the ADAMTS13 gene mutations.